SUPPORTING INFORMATION

N-Acyl L-homocysteine thiolactones are potent and stable synthetic modulators of the RhlR quorum sensing receptor in *Pseudomonas aeruginosa*

Michelle E. Boursier,[1,†] Joshua B. Combs,[1,‡] and Helen E. Blackwell[1,*]

[1]*Department of Chemistry, University of Wisconsin–Madison, 1101 University Ave., Madison, WI 53706, USA; blackwell@chem.wisc.edu*

Contents.

† *Current address:* Promega Corporation, Fitchburg, WI 53711

‡ *Current address:* Department of Chemistry, Yale University, New Haven, CT 06520

General chemical information

All chemical reagents and solvents were purchased from commercial sources and used without further purification, except for dichloromethane (DCM), which was distilled and dried over activated molecular sieves. Water (18 MΩ) was purified using a Thermo Scientific Barnstead Nanopure system. Chlorophenol red-β-D-galactopyranoside (CPRG) was purchased from Roche. *Ortho*-nitrophenyl-β-galactoside (ONPG) was purchased from Sigma Aldrich. All media and reagents for bacterial culture were purchased from standard commercial sources.

Instrumentation and analytical methods

NMR spectra were recorded in deuterated NMR solvents at 300 MHz on a Varian MercuryPlus 300 spectrometer, at 400 MHz on a Bruker Avance-400 spectrometer equipped with a SmartProbe and SampleJet, or at 500 MHz on a Bruker Avance-500 spectrometer equipped with a DCH cryoprobe and SampleXpress. Chemical shifts are reported in parts per million (ppm, δ) using corresponding solvents or tetramethylsilane (TMS) as a reference. Couplings are reported in hertz (Hz). Electrospray ionization MS measurements were performed on a Waters LCT. Samples were dissolved in acetonitrile and sprayed with a sample cone voltage of 20. For exact mass measurements (EMM), an aliquot of a known compound (lock mass) was added to the sample and resprayed.

Reversed-phase high performance liquid chromatography (RP-HPLC) was performed using a Shimadzu system equipped with a SCL-10Avp controller, a LC-20AT pump, a SIL-10AF autosampler, a CTO-20A oven, and a SPD-M20A UV/vis diode array detector. A Phenomenex Gemini C18 column (5 µm, 4.6 mm x 250 mm) was used for all analytical RP-HPLC work. Standard RP-HPLC conditions were as follows: flow rates were 1 mL min^{-1} for analytical separations; mobile phase A = 18 MΩ water + 0.1% TFA; mobile phase B = acetonitrile + 0.1% TFA. Purities were determined by integration of peaks with UV detection at 220 nm. For all RP-

HPLC analyses, the method was as follows: (i) start with isocratic 10% B (3 min), (ii) followed by a linear gradient from 10% to 95% B (27 min), and (iii) end with isocratic 95% B (2 min). Curves generated for compound stability studies were analyzed using a one-phase decay curve fit.

Fourier-transform infrared (FT-IR) spectra were recorded with a Bruker Tensor 27 IR spectrometer outfitted with a single reflection MIRacle Horizontal attenuated total reflectance (ATR) unit from Pike Technologies. A ZnSe crystal with spectral range 20,000 to 650 cm^{-1} was used for ATR-IR measurements.

Homocysteine thiolactone/homoserine lactone stability studies

Homocysteine thiolactone and homoserine lactone stability studies were performed as reported previously,[1] with the following modifications: compounds (50 μM) were dissolved in either 1 mM 2-(*N*-morpholino)ethanesulfonic acid (MES) buffer at pH 6, or 1 mM tris(hydroxymethyl)aminomethane (TRIS) buffer at pH 7, 8, or 9. Solutions were stored at room temperature, and 150 μL aliquots were removed every 2 h for 8 h, and then again at 24 h. Samples were immediately analyzed via RP-HPLC, and the area under the curve (AUC) at 220 nm was calculated and compared to the area at t = 0 h. Caffeine (50 μM) was added as an internal standard and maintained the same AUC throughout the assay (error ≤ 1–5%). Degradation of both compounds to the hydrolysis product was confirmed via mass spectrometry (MS) of the resulting byproduct peak (see Table S3 for MS data). The RP-HPLC traces are included directly after Table S3.

Compound characterization data

^{1}H- and ^{13}C-NMR, ESI MS, and IR data are reported below for all new compounds and select intermediates. Characterization data for compound **38** is included as it has not been fully characterized in past studies reporting this compound.[2] Copies of ^{1}H- and ^{13}C-NMR spectra are provided at the end of this document.

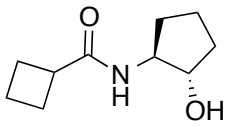

Alcohol precursor to **34**: ^{1}H NMR (400 MHz, $CDCl_3$) δ 5.71 (s, 1H), 4.80 (s, 1H), 3.91 (q, *J* = 6.7 Hz, 1H), 3.78 (ddt, *J* = 14.3, 8.8, 5.3 Hz, 1H), 3.00 (p, *J* = 8.5 Hz, 1H), 2.26 – 1.61 (m, 11H), 1.40 (dq, *J* = 12.8, 8.3 Hz, 1H); ^{13}C NMR (126 MHz, $CDCl_3$) δ 177.4, 80.0, 61.1, 39.7, 32.8, 30.7, 25.6, 25.5, 21.5, 18.2; Expected $[M+H]^+$: 184.1332, observed: 184.1331; IR (cm^{-1}): 3275, 2941, 2866, 1635, 1548, 1258, 685.

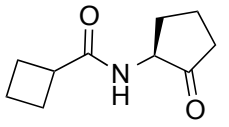

34: ^{1}H NMR (300 MHz, $CDCl_3$) δ 5.79 (s, 1H), 4.22 – 3.96 (m, 1H), 3.15 – 2.90 (m, 1H), 2.76 – 2.55 (m, 1H), 2.47 – 1.76 (m, 11H), 1.57 (qd, *J* = 12.3, 6.9 Hz, 1H); ^{13}C NMR (101 MHz, $CDCl_3$) δ 215.6, 175.5, 58.2, 39.7, 35.1, 30.4, 25.5, 25.4, 18.3, 18.2; Expected $[M+H]^+$: 182.1176, observed: 182.1176; IR (cm^{-1}): 3250, 2923, 2859, 1742, 1635, 1548, 1270.

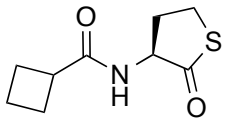

35: ^{1}H NMR (400 MHz, $CDCl_3$) δ 6.08 (d, 1H), 4.51 (dt, *J* = 13.1, 6.7 Hz, 1H), 3.33 (td, *J* = 11.8, 5.2 Hz, 1H), 3.21 (dd, *J* = 11.1, 6.7 Hz, 1H), 3.04 (p, *J* = 8.5 Hz, 1H), 2.92 – 2.78 (m, 1H), 2.34 – 2.06 (m, 4H), 2.00 – 1.76 (m, 3H); ^{13}C NMR (126 MHz, $CDCl_3$) δ 205.8, 175.6, 59.6, 39.8, 32.4, 27.8, 25.5, 25.5,18.3; Expected $[M+H]^+$: 200.0740, observed: 200.0739; IR (cm^{-1}): 3250, 2975, 2933, 1686, 1637, 1552, 1257, 913.

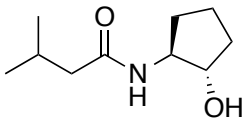

Alcohol precursor to **36**: ^{1}H NMR (500 MHz, $CDCl_3$) δ 5.56 (s, 1H), 4.60 (s, 1H), 3.95 (q, *J* = 6.4 Hz, 1H), 3.89 – 3.73 (m, 1H), 2.19 – 1.97 (m, 5H), 1.80 (dtdd, *J* = 12.5, 9.2, 6.4, 2.7 Hz, 1H), 1.75 – 1.62 (m, 2H), 1.41 (dq, *J* = 12.8, 8.3 Hz, 1H), 0.97 (dd, *J* = 6.3, 1.0 Hz, 6H); ^{13}C NMR (126 MHz, $CDCl_3$) δ 175.0, 80.1, 61.2, 45.8, 32.8, 30.8, 26.4, 22.6, 22.5, 21.6; Expected $[M+H]^+$: 186,1489, observed: 186.1487; IR (cm^{-1}): 3286, 3088, 2953, 2925, 2867, 1636, 1551, 1049.

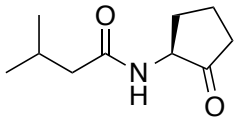

36: ^{1}H NMR (300 MHz, $CDCl_3$) δ 5.84 (s, 1H), 4.24 – 3.98 (m, 1H), 2.66 (dddd, *J* = 14.0, 7.9, 3.7, 1.6 Hz, 1H), 2.49 – 2.34 (m, 1H), 2.27 – 1.99 (m, 5H), 1.86 (tddd, *J* = 13.0, 10.7, 8.9, 6.1 Hz, 1H), 1.58 (qd, *J* = 12.3, 6.9 Hz, 1H), 0.95 (dd, *J* = 6.5, 3.2 Hz, 5H); ^{13}C NMR (126 MHz, $CDCl_3$) δ 215.4, 173.0, 58.3, 45.8, 35.0, 30.3, 26.3, 22.6, 22.5, 18.2; Expected $[M+H]^+$: 184.1332, observed: 184.1331; IR (cm^{-1}): 3256, 3073, 2958, 2869, 1748, 1637, 1550, 1372.

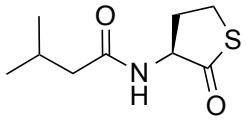

37: ^{1}H NMR (300 MHz, $CDCl_3$) δ 6.04 (s, 1H), 4.53 (dt, *J* = 12.9, 6.5 Hz, 1H), 3.35 (td, *J* = 11.7, 5.1 Hz, 1H), 3.29 – 3.16 (m, 1H), 2.99 – 2.83 (m, 1H), 2.08 (d, *J* = 6.5 Hz, 3H), 1.91 (qd, *J* = 12.4, 7.0 Hz, 1H), 1.00 – 0.88 (m, 6H); ^{13}C NMR (126 MHz, $CDCl_3$) δ 205.8, 173.1, 59.5, 45.8, 32.2, 27.7, 26.3, 22.6, 22.5; Expected $[M+H]^+$: 202.0896, observed: 202.0893; IR (cm^{-1}): 3267, 3071, 2952, 2924, 2866, 1690, 1638, 1548, 917.

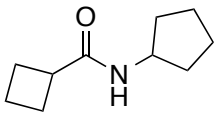

38: ^{1}H NMR (400 MHz, $CDCl_3$) δ 5.81 (d, 1H), 4.09 (h, *J* = 7.1 Hz, 1H), 2.91 (p, *J* = 8.4 Hz, 1H), 2.18 (pd, *J* = 9.2, 2.3 Hz, 2H), 2.07 – 1.95 (m, 2H), 1.94 – 1.68 (m, 4H), 1.66 – 1.40 (m, 4H), 1.28 (dq, *J* = 14.1, 7.5, 7.0 Hz, 2H); ^{13}C NMR (126 MHz, $CDCl_3$) δ 174.6, 51.1, 40.2, 33.4, 25.5, 23.9, 18.2; Expected $[M+H]^+$: 168.1383, observed: 168.1381; IR (cm^{-1}): 3290, 2946, 2865, 1636, 1545,1257, 678.

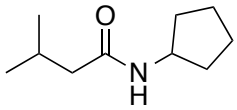

39: ^{1}H NMR (500 MHz, $CDCl_3$) δ 5.31 (d, *J* = 10.9 Hz, 1H), 4.22 (h, *J* = 7.0 Hz, 1H), 2.10 (dp, *J* = 13.2, 6.6 Hz, 1H), 2.03 – 1.94 (m, 4H), 1.71 – 1.54 (m, 4H), 1.42 – 1.28 (m, 2H), 0.94 (d, *J* = 6.6 Hz, 6H); ^{13}C NMR (126 MHz, $CDCl_3$) δ 172.1, 51.2, 46.5, 33.4, 26.4, 23.8, 22.6; Expected $[M+H]^+$: 170.1539, observed: 170.1537; IR (cm^{-1}): 297, 3073, 2954, 2868, 1633, 1541.

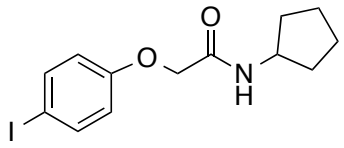

40: ^{1}H NMR (400 MHz, $CDCl_3$) δ 7.59 (d, *J* = 8.7 Hz, 2H), 6.70 (d, *J* = 8.7 Hz, 2H), 6.39 (s, 1H), 4.42 (s, 2H), 4.29 (h, *J* = 7.0 Hz, 1H), 2.01 (dd, *J* = 12.4, 5.7 Hz, 2H), 1.66 (dt, *J* = 19.4, 7.9 Hz, 4H), 1.41 (dd, *J* = 12.6, 6.3 Hz, 2H); ^{13}C NMR (101 MHz, $CDCl_3$) δ 167.2, 157.2, 138.7, 117.1, 84.6, 67.6, 50.9, 33.1, 23.8; Expected $[M+H]^+$: 346.0299, observed: 346.0290; IR (cm^{-1}): 3271, 2925, 2865, 1647, 1553, 1482, 1453, 1234, 843.

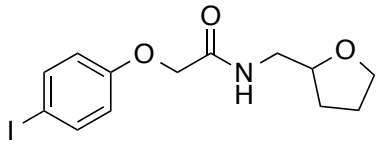

41 (prepared and evaluated as the racemate): ^{1}H NMR (500 MHz, $CDCl_3$) δ 7.60 – 7.53 (m, 2H), 6.88 – 6.77 (m, 1H), 6.75 – 6.66 (m, 2H), 4.46 (s, 2H), 3.98 (qd, *J* = 7.1, 3.4 Hz, 1H), 3.86 – 3.69 (m, 2H), 3.61 (ddd, *J* = 13.8, 6.4, 3.4 Hz, 1H), 3.32 – 3.21 (m, 1H), 2.01 – 1.90 (m, 1H), 1.86 (dq, *J* = 14.0, 6.9, 6.4 Hz, 2H), 1.51 (dq, *J* = 12.1, 7.6 Hz, 1H); ^{13}C NMR (126 MHz, $CDCl_3$) δ 167.9, 157.2, 138.7, 117.1, 84.5, 77.6, 68.4, 67.5, 42.7, 28.7, 26.0; Expected $[M+H]^+$: 362.0248, observed 362.0241; IR (cm^{-1}): 3277, 2969, 2924, 2864, 1655, 1547, 1481, 1240, 1058.

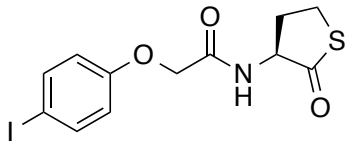

42: ^{1}H NMR (500 MHz, $CDCl_3$) δ 7.70 – 7.48 (m, 2H), 6.94 (d, *J* = 7.6 Hz, 1H), 6.77 – 6.68 (m, 2H), 4.61 (dt, *J* = 13.2, 6.7 Hz, 1H), 4.50 (d, *J* = 2.6 Hz, 2H), 3.39 (td, *J* = 11.8, 5.1 Hz, 1H), 3.32 – 3.27 (m, 1H), 3.02 – 2.88 (m, 1H), 2.01 (qd, *J* = 12.4, 7.0 Hz, 1H); ^{13}C NMR (126 MHz, $CDCl_3$) δ 204.7, 168.4, 157.0, 138.8, 117.2, 84.9, 67.4, 59.1, 31.8, 27.7; Expected $[M+H]^+$: 377.9655, observed: 377.9650; IR (cm^{-1}): 3282, 2974, 2926, 2858, 1696, 1655, 1536, 1233.

Supplementary reporter assay data and analysis

Table S1. Complete primary agonism and antagonism data for BHL and AHL analogs in the *E. coli* RhlR reporter strain.[a]

Compound	% RhlR activation (10 μM)[b]	% RhlR activation (1 mM)[c]	% RhlR inhibition (10 μM)[d]	% RhlR inhibition (1 mM)[e]
BHL	51	100	–	–
S4	76	94	-52	-95
34	56	100	-39	-98
35	88	100	-85	-110
36	42	84	-35	-120
37	85	92	-59	-81
38	0	34	24	25
39	0	20	11	31
40[f]	1	1	6	24
41	0	0	6	61
42	1	7	28	74

[a]Assays performed using the *E. coli* RhlR reporter strain JLD271/pJN105R2/pSC11-*rhlI**. SEM of n ≥ 3 trials did not exceed ± 10%. [b]Compounds screened at 10 μM. RhlR activity measured relative to that of 1 mM BHL. [c]Compounds screened at 1 mM. RhlR activity measured relative to that of 1 mM BHL. [d]Compounds screened at 10 μM in the presence of 10 μM BHL. Negative values indicate agonism stronger than that of 10 μM BHL alone. [e]Compounds screened at 1 mM in the presence of 10 μM BHL. Negative values indicate agonism stronger than that of 10 μM BHL alone. [f]Screened at a maximal concentration of 100 μM due to reduced solubility at higher concentrations.

Table S2. Complete primary agonism and antagonism data for BHL, OdDHL, and AHL analogs in the *E. coli* LasR reporter strain.[a]

Compound	% LasR activation (10 μM)[b]	% LasR activation (1 mM)[c]	% LasR inhibition (10 μM)[d]	% LasR inhibition (1 mM)[e]
BHL	1	6	-2	35
OdDHL[f]	100	100	–	–
S4	6	21	19	32
34	0	15	16	60
35	0	10	18	63
36	0	0	-7	53
37	0	7	25	63
38	0	0	-2	22
39	1	1	-2	13
40[f]	3	1	11	2
41	11	0	-16	58
42	35	53	18	-14

[a]Assays performed using the *E. coli* LasR reporter strain JLD271/pJN105L/pSC11. SEM of n ≥ 3 trials did not exceed ± 10%. [b]Compounds screened at 10 μM. LasR activity measured relative to that of 100 μM OdDHL. [c]Compounds screened at 1 mM. LasR activity measured relative to that of 100 μM OdDHL. [d]Compounds screened at 10 μM in the presence of 2 nM OdDHL. Negative values indicate agonism stronger than that of 2 nM OdDHL alone. [e]Compounds screened at 1 mM in the presence of 2 nM OdDHL. Negative values indicate agonism stronger than that of 2 nM OdDHL alone. [f]Screened at a maximal concentration of 100 μM due to reduced solubility at higher concentrations.

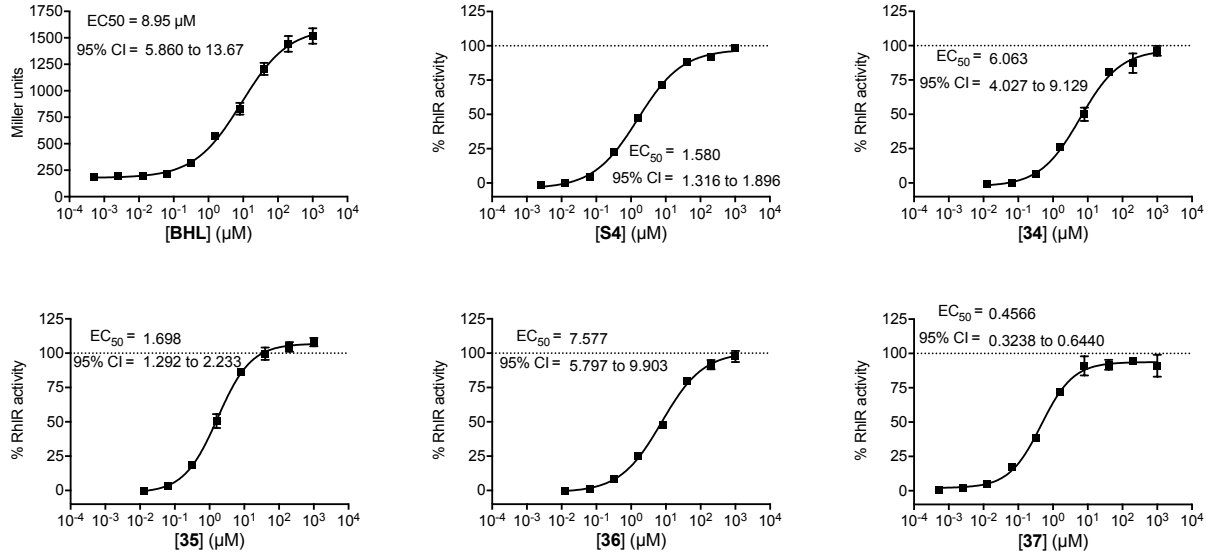

Figure S1. Dose-response curves for RhlR agonism in the *E. coli* reporter by BHL and lead compounds. Assay performed using the *E. coli* JLD271/pJN105R2/pSC11-*rhlI** reporter strain. % Activity defined as the activity of the compound relative to maximum possible RhlR activity (i.e., activity effected by BHL at 1 mM). EC_{50} values and 95% Confidence Intervals (CI; shown on each plot in μM) calculated using GraphPad Prism. Error bars, SEM of n ≥ 3 trials.

Note S1. Comments on Hill slopes for RhlR agonist dose response curves in the *E. coli* and *P. aeruginosa* reporter strains.

The dose-response curves of **BHL** and **S4** are shallower (Hill slope = 0.7) in the *E. coli* RhlR reporter strain (Hill slope = ~1.0) than curves for other AHL ligands in related LuxR-type receptor reporter strains (Figure S1). Shallow dose-response curves are often indicative of negative cooperativity, with the small molecule binding to multiple sites on the receptor.[3] Since RhlR functions as a dimer, this negative cooperativity scenario is feasible if binding of an agonist to RhlR reduces the binding affinity of the second dimer site for the agonist.

For compounds **34** and **36**, the Hill slopes in the dose-response agonism curves remained similar to that of previous agonists (~0.7). However, thiolactones **35** and **37** displayed slopes much closer to ~1.0. As the latter slope is more typical for LuxR-type receptor-ligand binding, it is plausible the thiolactone hybrids are not reducing the binding affinity of the second dimer site. Further studies are required to determine whether this different Hill slope is representative of a unique mechanism of action. Additionally, all dose-response curves in the *P. aeruginosa* RhlR reporter had Hill slopes much closer to 1.0 (Figure S2), suggesting that the shallow dose-response curves observed in the *E. coli* RhlR reporter may simply be artifacts of heterologous expression.

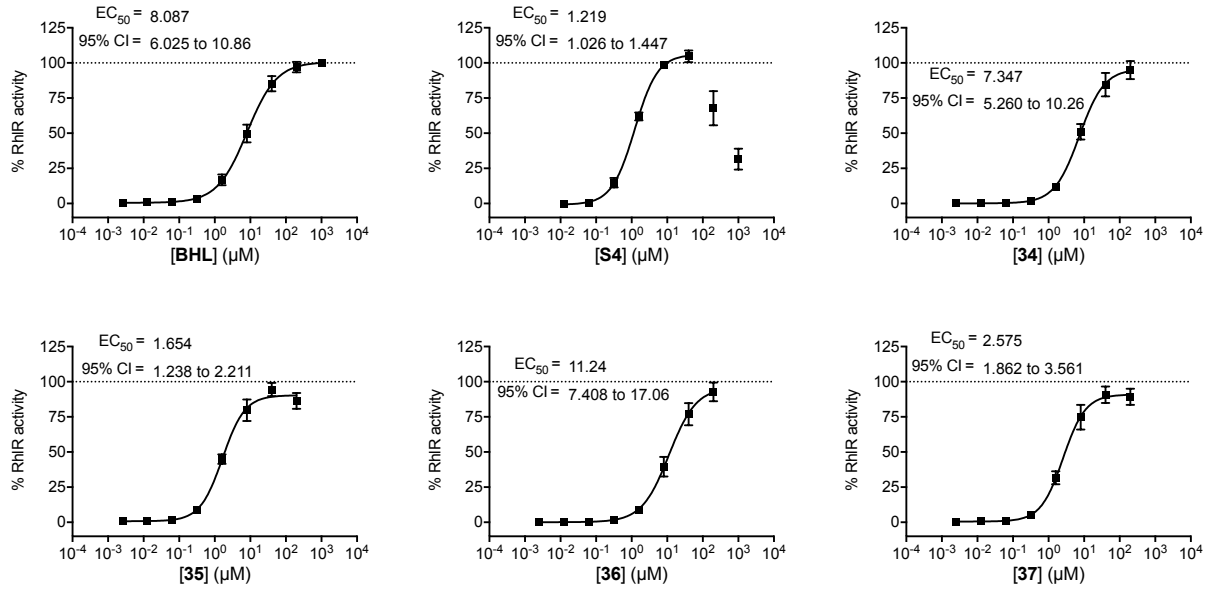

Figure S2. Dose-response curves for RhlR agonism in the *P. aeruginosa* reporter by BHL and lead compounds. Assays performed using the *P. aeruginosa* PAO-JP2/p*rhlI*-LVA*gfp* reporter strain. % Activity defined as the activity of the compound relative to maximum possible RhlR activity (i.e., activity effected by BHL at 1 mM). For compound **S4**, the EC_{50} value was calculated from the region of the dose-response curve that indicated RhlR agonism. EC_{50} values and associated 95% Confidence Intervals (CI; shown on each plot in μM) calculated using GraphPad Prism. Error bars, SEM of n ≥ 3 trials.

Note S2. Comments on non-monotonic dose response curve for compound **S4**, a RhlR agonist in *P. aeruginosa*.

We note that compound **S4** displays non-monotonic dose behavior in the *P. aeruginosa* RhlR reporter (i.e., a dose-response curve that increases in activity at low concentrations, followed by a decrease in activity at high concentrations—often referred to as an “inverted U-shape” curve; Figure S2). Ongoing studies are focused on determining the origin(s) of this phenomenon. Note, we do not believe this behavior is due to **S4** toxicity or insolubility at high concentrations. Hybrid compounds **34**–**37**, each with a non-native head group, do not display such non-monotonic dose curves, suggesting that the nature of the head group may contribute to this alternate behavior in the *P. aeruginosa* RhlR reporter.

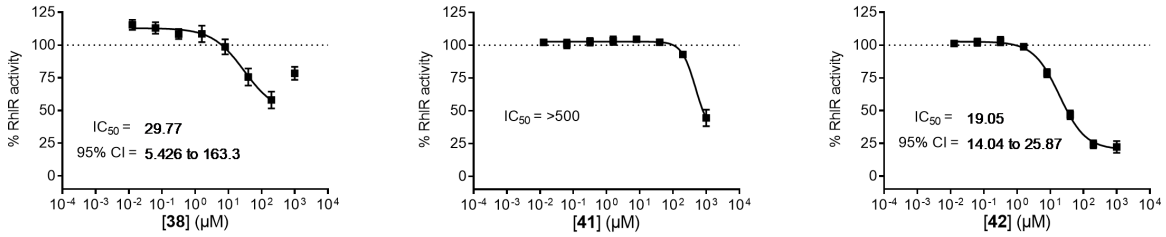

Figure S3. Dose-response curves for RhlR antagonism in the *E. coli* reporter by lead compounds. Assay performed using the *E. coli* JLD271/pJN105R2/pSC11-*rhlI** reporter strain with the addition of 10 μM BHL. % Activity defined as the activity of the compound relative to half maximal RhlR activity (i.e., activity effected by BHL at 10 μM). For compound **38**, the IC_{50} value was calculated from the region of the dose-response curve that indicated RhlR antagonism. IC_{50} values and 95% Confidence Intervals (CI; shown on each plot) calculated using GraphPad Prism. Error bars, SEM of n ≥ 3 trials.

Note S3. Comments on dose response curve for compound **38**, a RhlR antagonist in *E. coli*.

We note that compound **38** displays (i) a high baseline activity (>100%) at low concentrations and (ii) non-monotonic dose behavior (i.e., a dose-response curve that decreases in activity at low concentrations, followed by an increase in activity at high concentrations; Figure S3) in the *E. coli* RhlR reporter. We have previously described the latter behavior for AHL-derived antagonists of RhlR and other LuxR-type receptors examined using similar reporter systems.[4, 5] Ongoing studies are focused on determining the origin(s) of these phenomena for compound **38**.

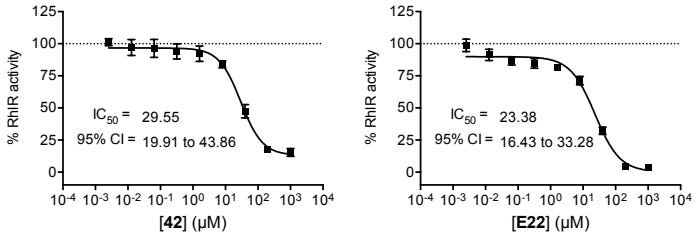

Figure S4. Dose-response curves for RhlR antagonism in the *P. aeruginosa* reporter by lead compounds. Assays performed using the *P. aeruginosa* PAO-JP2/p*rhlI*-LVA*gfp* reporter strain with the addition of 10 μM BHL. % Activity defined as the activity of the compound relative to half maximal RhlR activity (i.e., activity effected by BHL at 10 μM). IC_{50} values and associated 95% Confidence Intervals (CI; shown on each plot) calculated using GraphPad Prism. Error bars, SEM of n ≥ 3 trials.

MS data from compound stability studies

Table S3. MS data for compound hydrolysis products collected via RP-HPLC.

Compound	Expected $[M-H]^-$	Observed
E22	393.9615	393.9613
42	377.9844	377.9845

HPLC traces from compound stability studies

Compound **E22** at pH 6.

Caffeine retention time (t_R): 12.1 min; **E22** t_R: 22.5 min; hydrolysis product t_R: 19.6 min

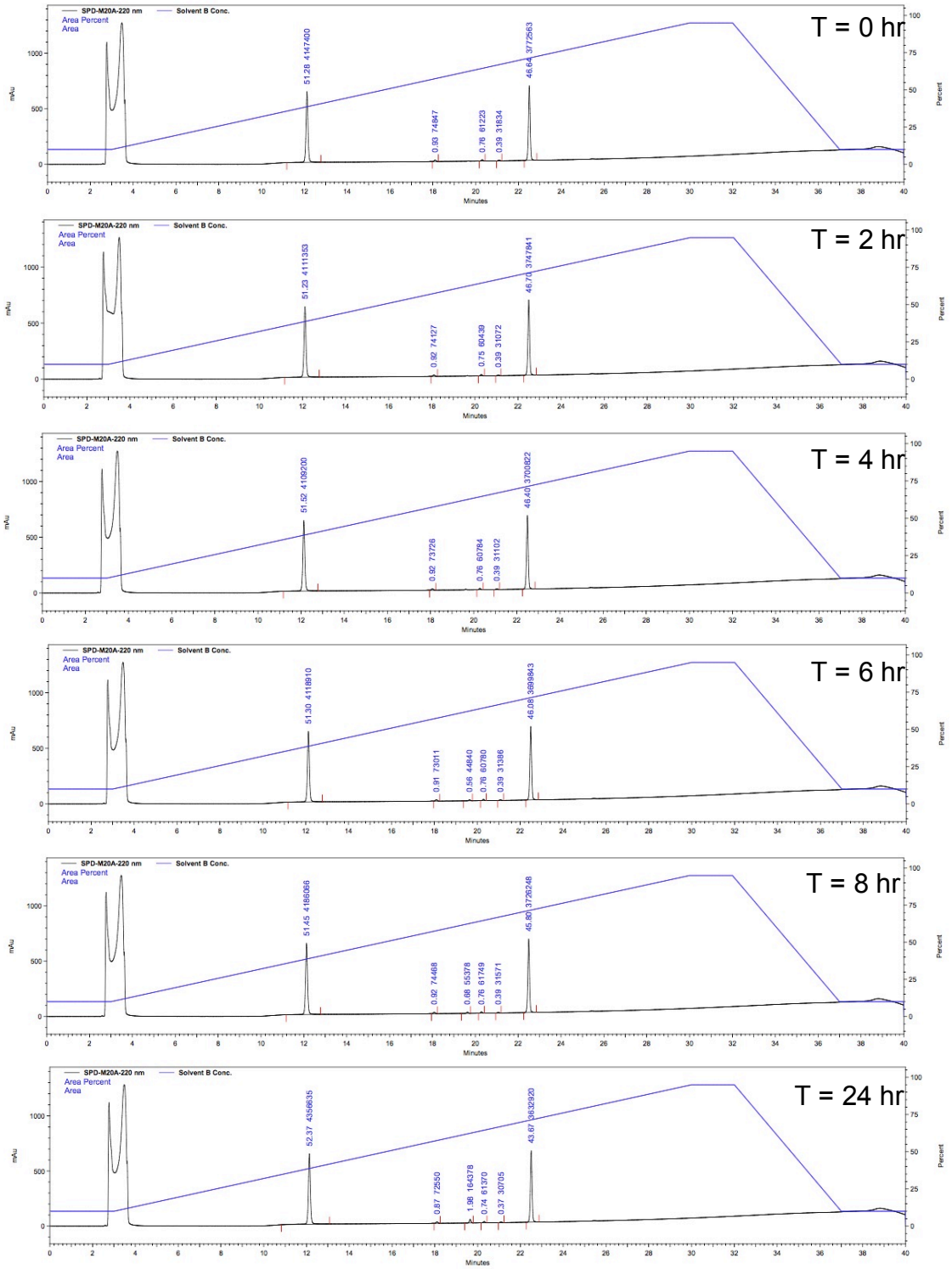

Time	0 hr	2 hr	4 hr	6 hr	8 hr	24 hr
% Remaining	100	100	99	99	98	92

Compound **42** at pH 6.

Caffeine t_R: 12.1 min; **42** t_R: 24.7 min; hydrolysis product t_R: 23.5 min

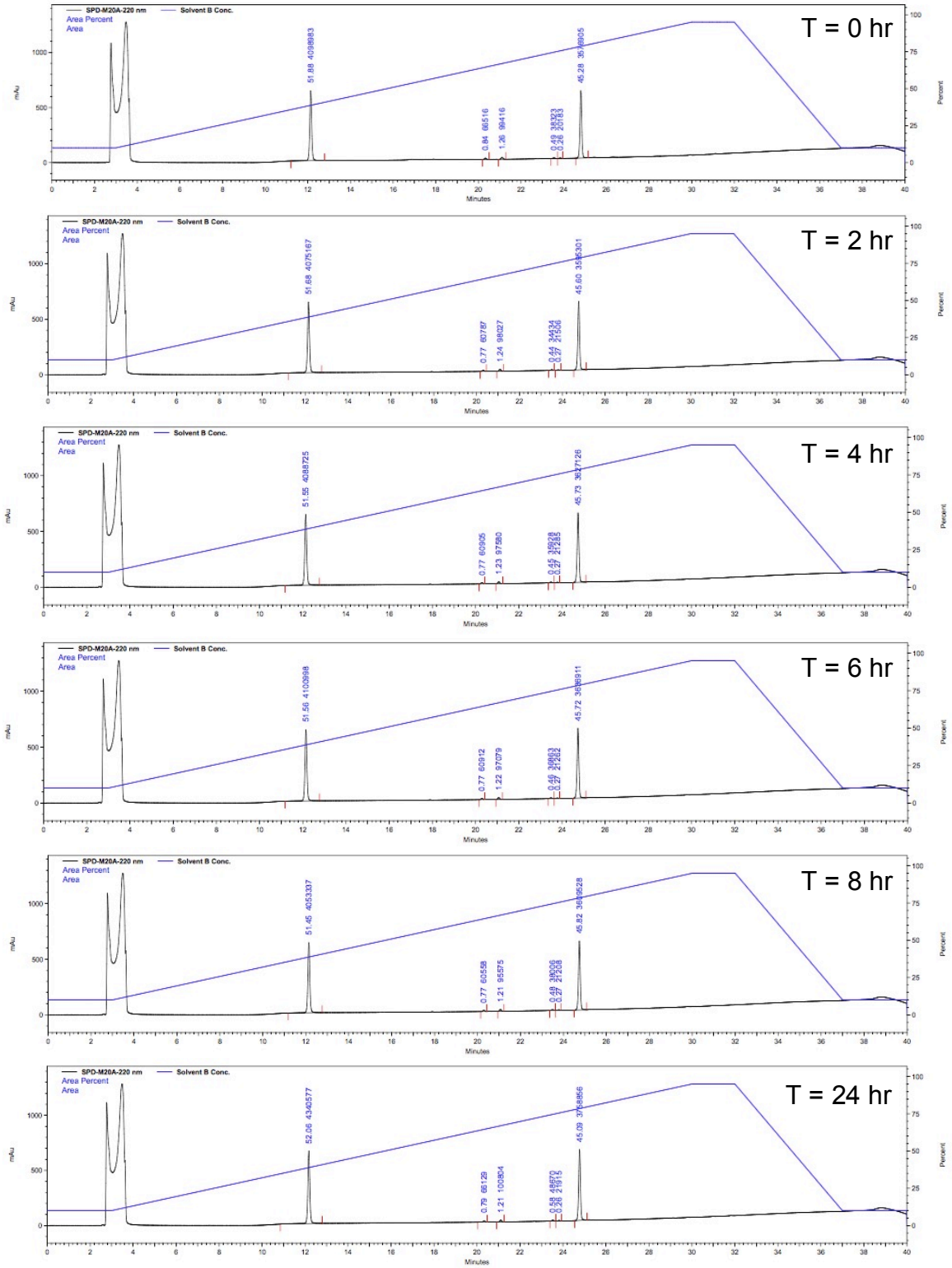

Time	0 hr	2 hr	4 hr	6 hr	8 hr	24 hr
% Remaining	100	100	100	100	100	99

Compound **E22** at pH 7.

Caffeine t_R: 12.1 min; **E22** t_R: 22.5 min; hydrolysis product t_R: 19.6 min

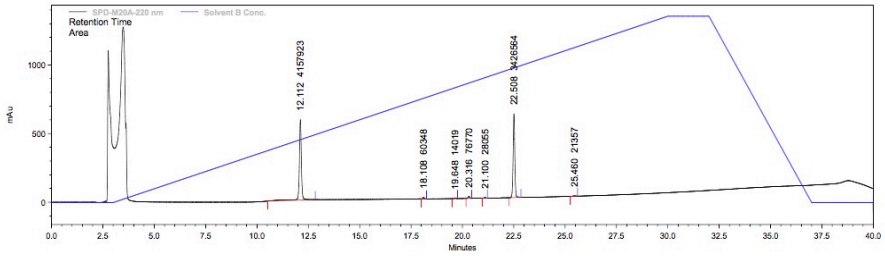

T = 0 hr

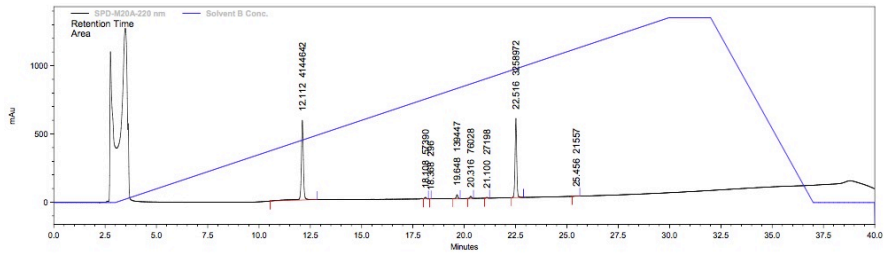

T = 2 hr

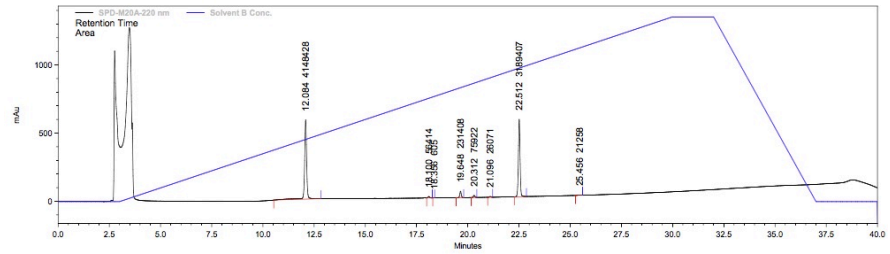

T = 4 hr

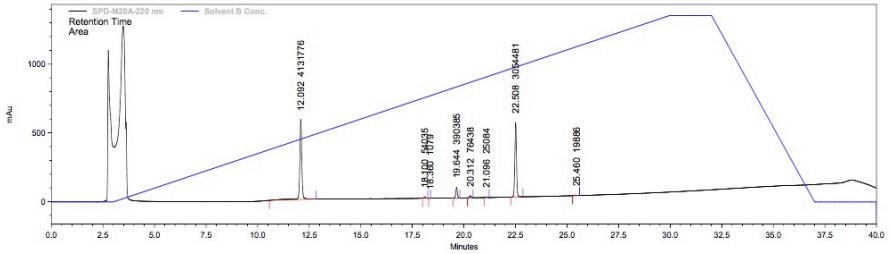

T = 6 hr

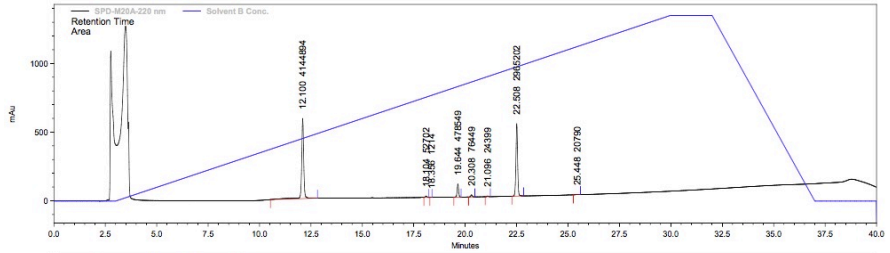

T = 8 hr

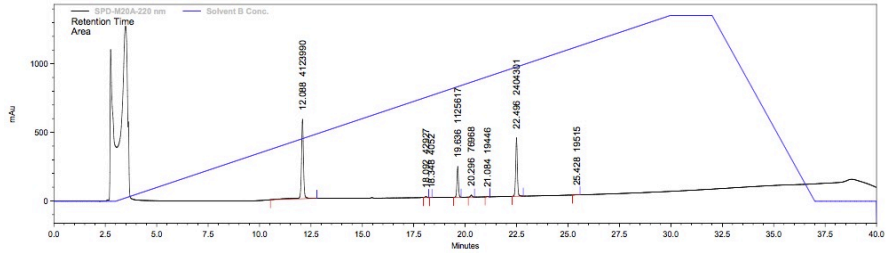

T = 24 hr

Time	0 hr	2 hr	4 hr	6 hr	8 hr	24 hr
% Remaining	100	95	93	89	87	70

Compound **42** at pH 7.

Caffeine t_R: 12.1 min; **42** t_R: 24.7 min; hydrolysis product t_R: 23.5 min

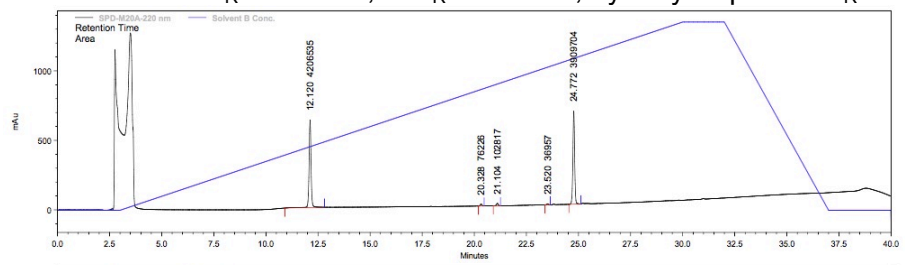

T = 0 hr

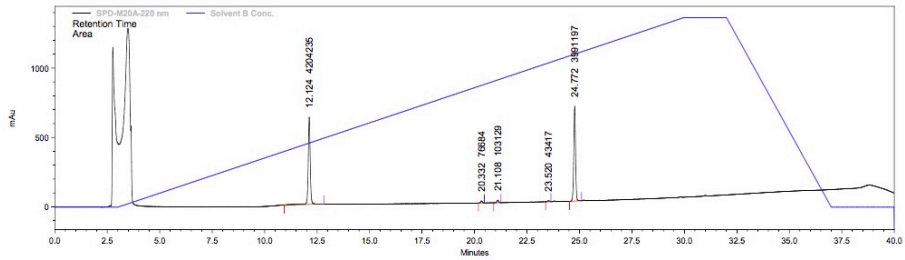

T = 2 hr

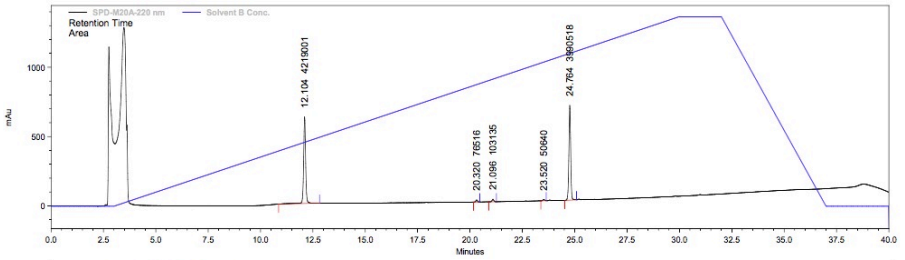

T = 4 hr

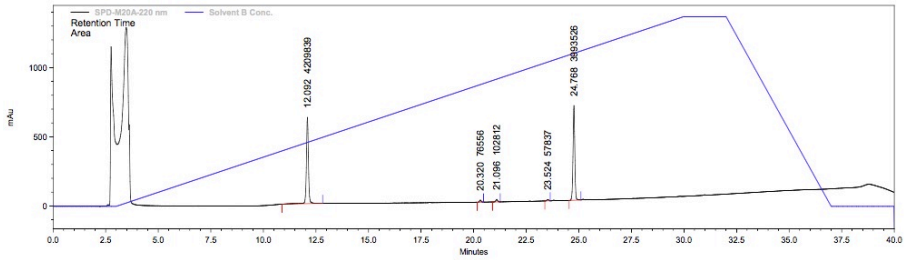

T = 6 hr

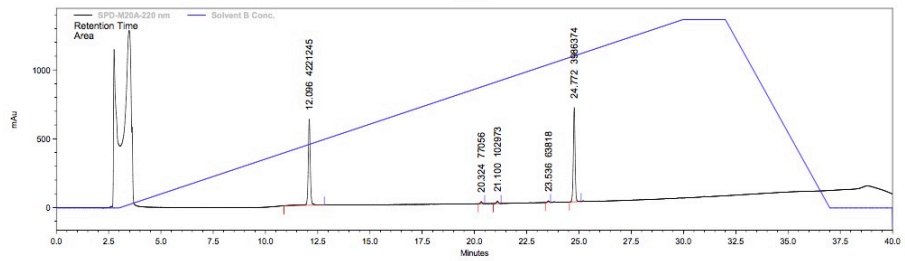

T = 8 hr

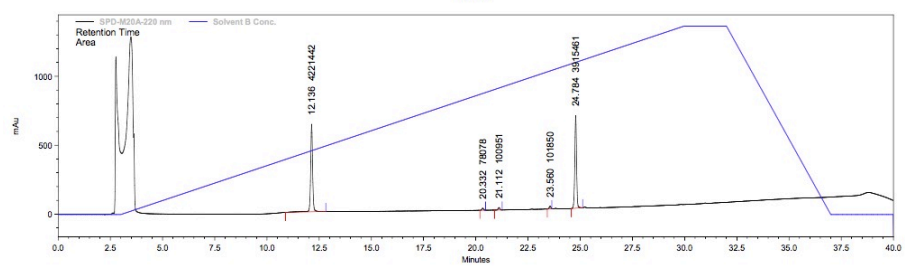

T = 24 hr

Time	0 hr	2 hr	4 hr	6 hr	8 hr	24 hr
% Remaining	100	100	100	100	100	100

Compound **E22** at pH 8.

Caffeine t_R: 12.1 min; **E22** t_R: 22.5 min; hydrolysis product t_R: 19.6 min

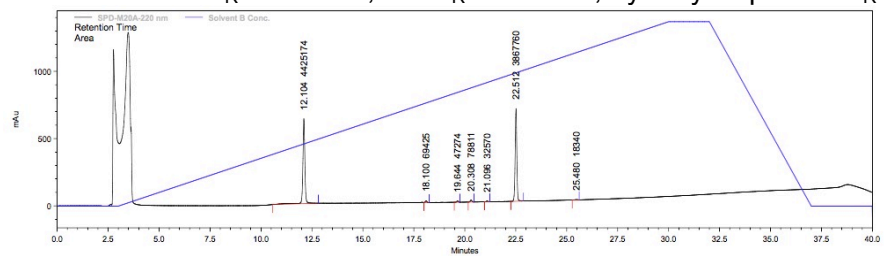

T = 0 hr

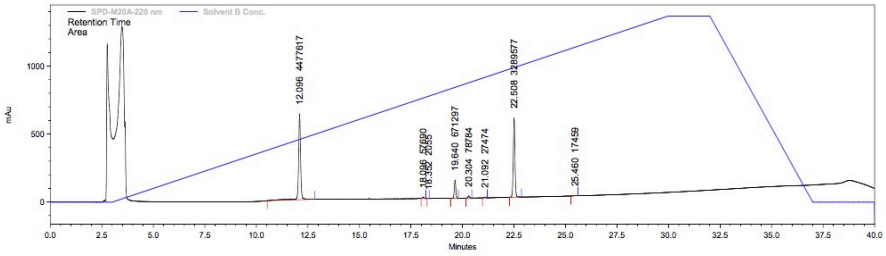

T = 2 hr

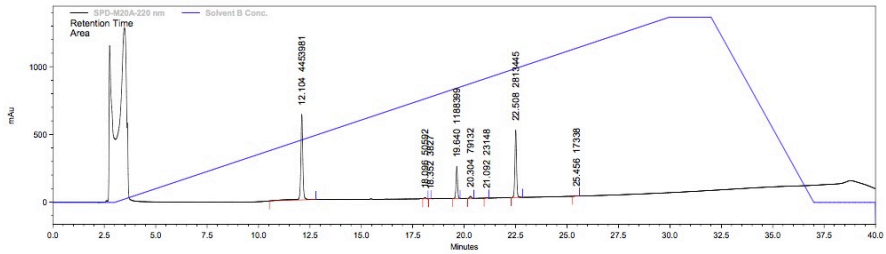

T = 4 hr

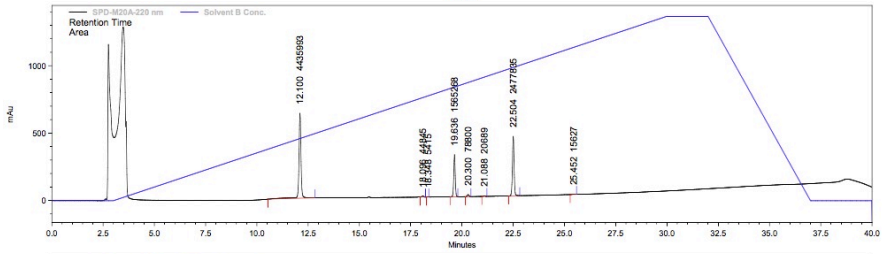

T = 6 hr

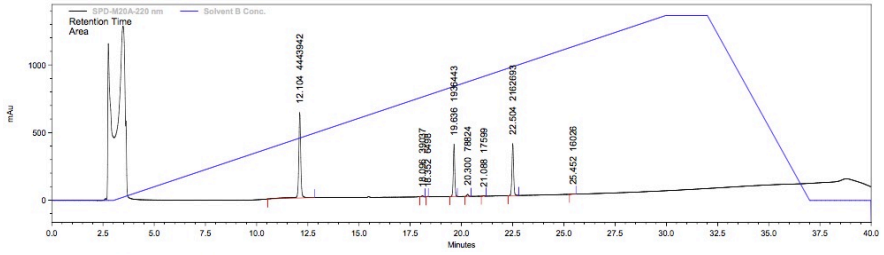

T = 8 hr

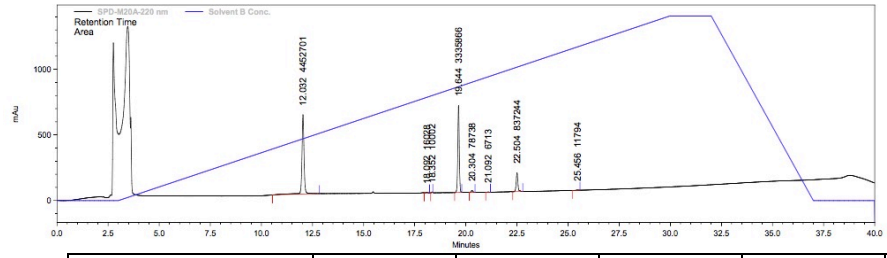

T = 24 hr

Time	0 hr	2 hr	4 hr	6 hr	8 hr	24 hr
% Remaining	100	85	73	64	56	22

Compound **42** at pH 8.

Caffeine t_R: 12.1 min; **42** t_R: 24.7 min; hydrolysis product t_R: 23.5 min

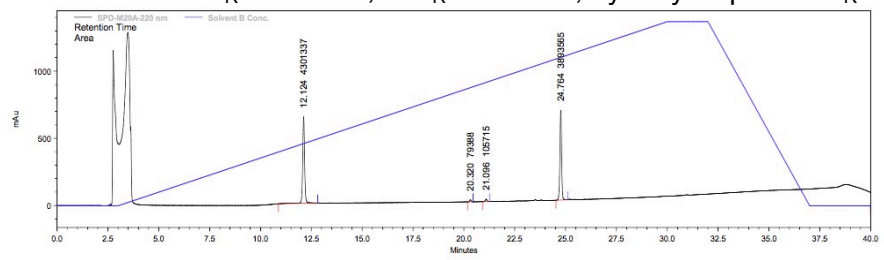

T = 0 hr

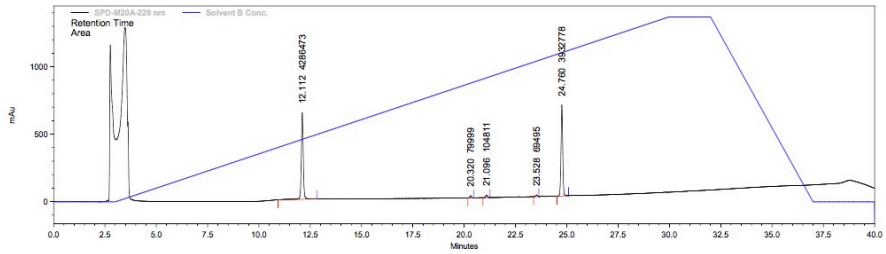

T = 2 hr

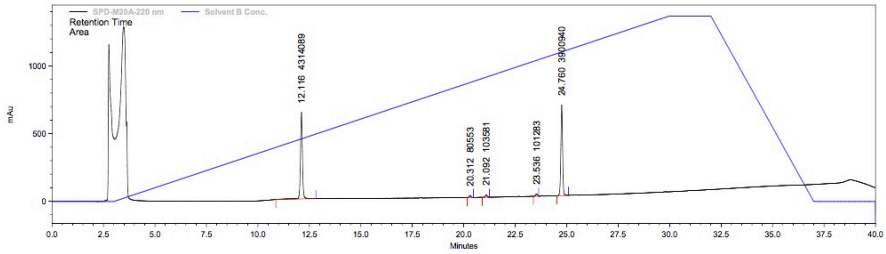

T = 4 hr

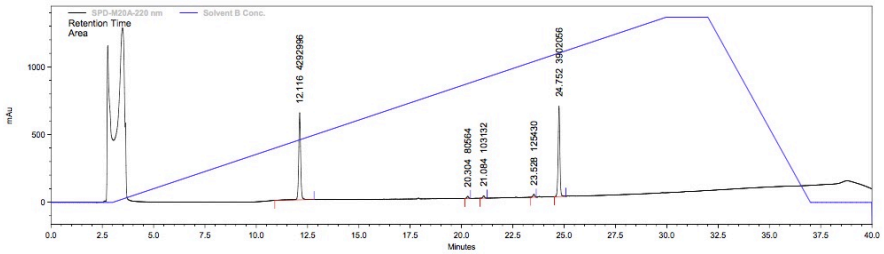

T = 6 hr

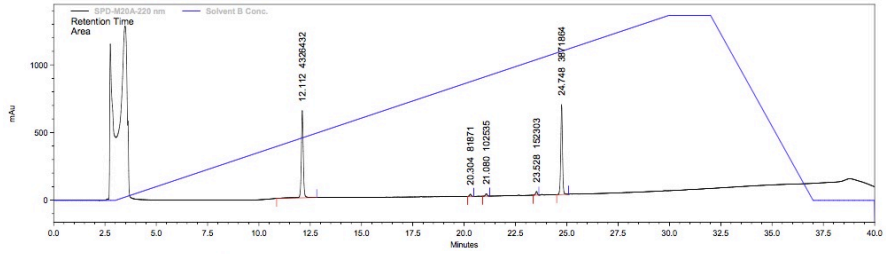

T = 8 hr

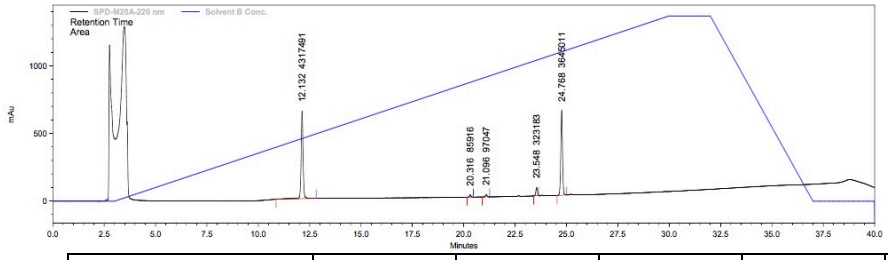

T = 24 hr

Time	0 hr	2 hr	4 hr	6 hr	8 hr	24 hr
% Remaining	100	100	100	100	99	94

Compound **E22** at pH 9.

Caffeine t_R: 12.1 min; **E22** t_R: 22.5 min; hydrolysis product t_R: 19.6 min

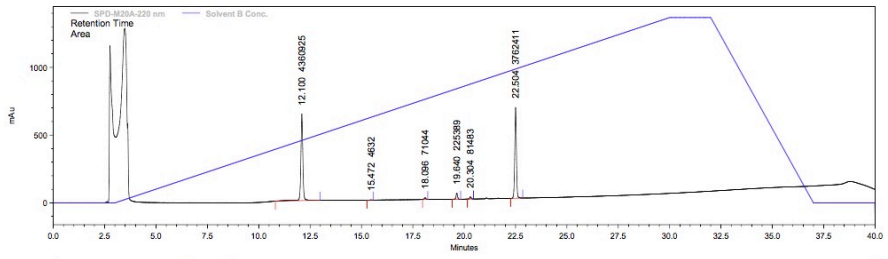

T = 0 hr

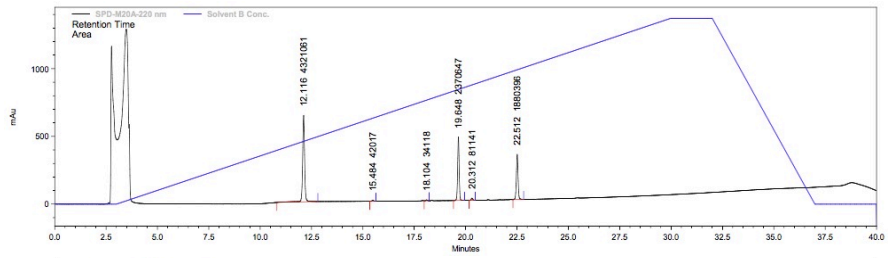

T = 2 hr

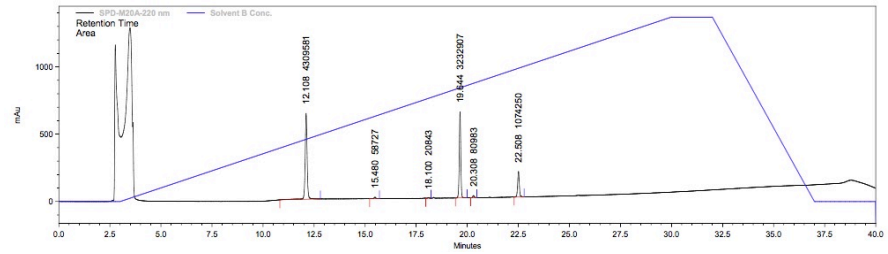

T = 4 hr

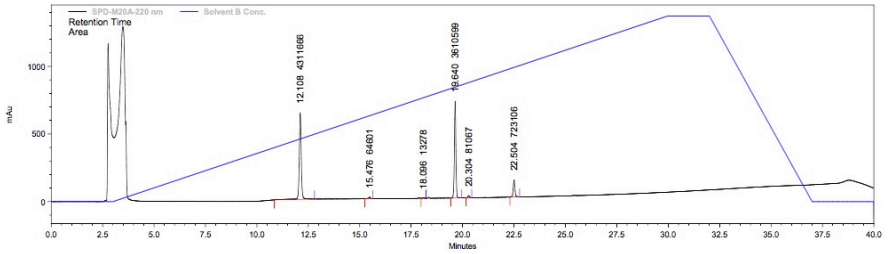

T = 6 hr

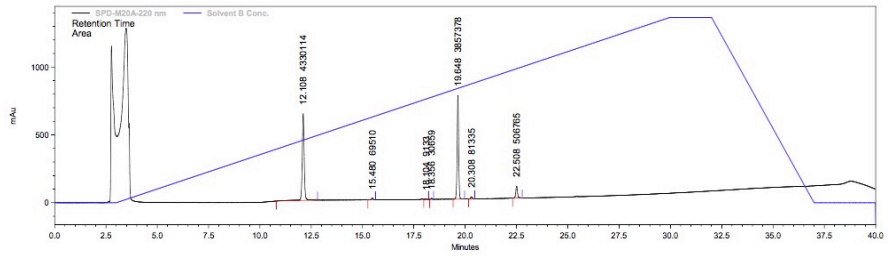

T = 8 hr

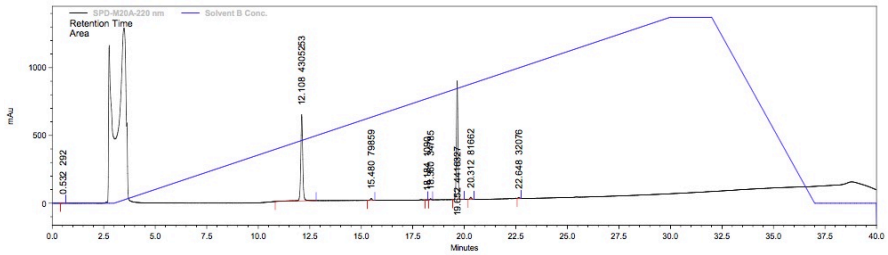

T = 24 hr

Time	0 hr	2 hr	4 hr	6 hr	8 hr	24 hr
% Remaining	100	50	29	19	13	0

Compound **42** at pH 9.

Caffeine t_R: 12.1 min; **42** t_R: 24.7 min; hydrolysis product t_R: 23.5 min

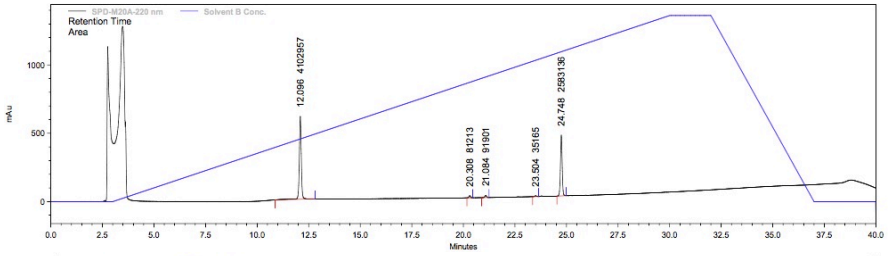

T = 0 hr

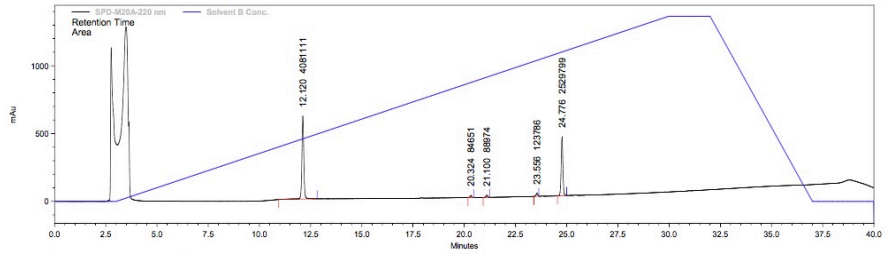

T = 2 hr

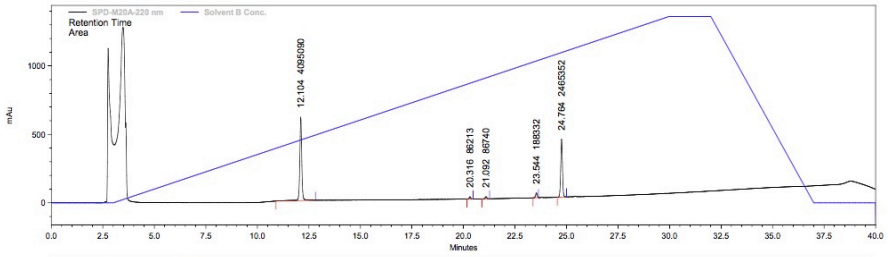

T = 4 hr

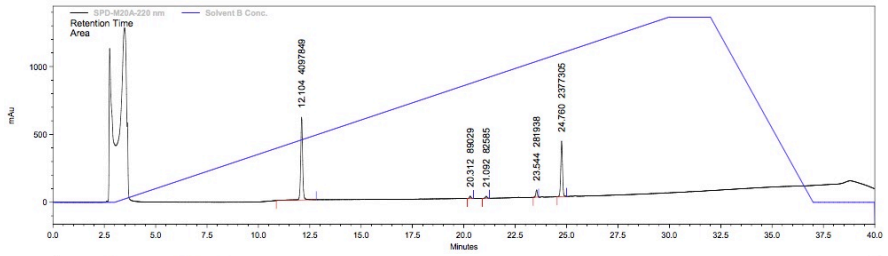

T = 6 hr

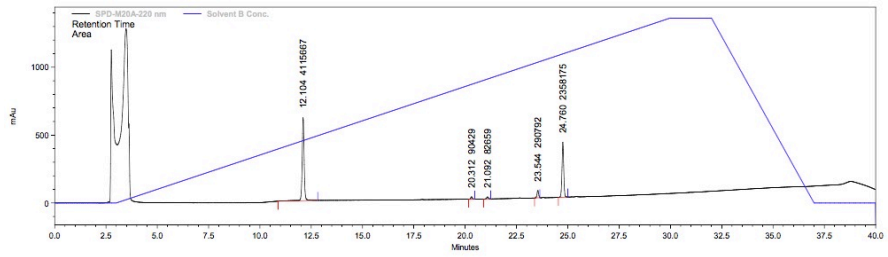

T = 8 hr

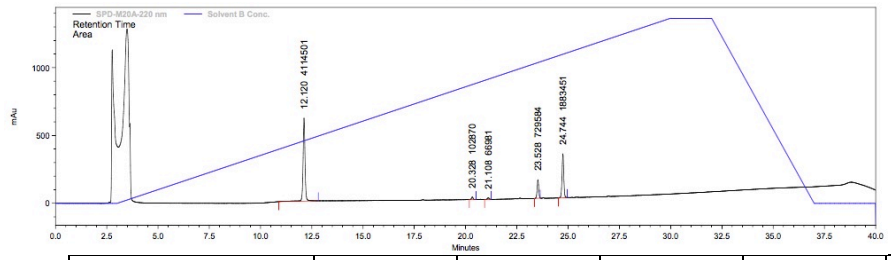

T = 24 hr

Time	0 hr	2 hr	4 hr	6 hr	8 hr	24 hr
% Remaining	100	97	95	92	91	73

^{1}H- and ^{13}C-NMR spectra

/Users/michelleboursier/Desktop/D1508121335_MEB_2.187P/10/fid

6.081 4.925 3.881 3.866 3.743 3.735 3.029 3.008 2.987 2.965 2.944 2.640 2.264 2.242 2.220 2.197 2.175 2.091 2.086 2.070 2.041 1.962 1.935 1.917 1.895 1.890 1.873 1.869 1.865 1.839 1.813 1.809 1.807 1.791 1.784 1.769 1.756 1.746 1.736 1.733 1.724 1.714 1.689 1.685 1.663 1.636 1.616 1.606 1.598 1.595 1.433 1.412 1.399 1.391 1.381 1.372 1.360 1.338

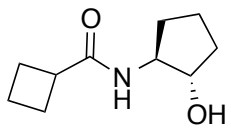

Precursor to 34

C1509091044_MEB_RN12OH.11.fid — Group Blackwell — C13CPD32 CDCl3 /home/mboursier/callisto mboursier 3

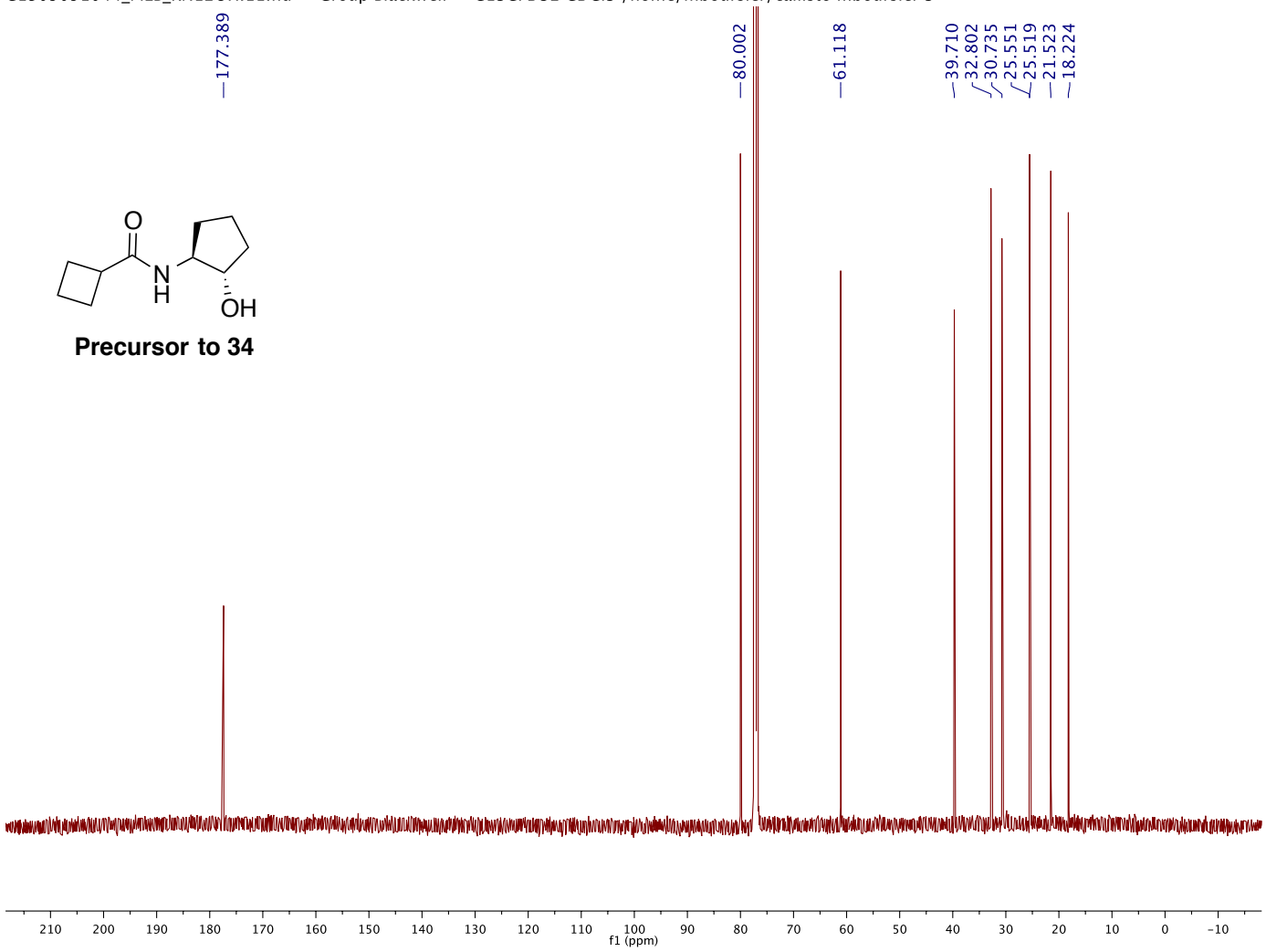

Precursor to 34

D1509080935_MEB_2.201_12-17.10.fid — Group Blackwell — PROTON CDCl3 /home/mboursier/av400 mboursier 51

5.852 4.093 4.078 4.062 4.045 4.046 3.025 3.004 2.637 2.622 2.607 2.430 2.428 2.408 2.382 2.379 2.359 2.357 2.291 2.284 2.274 2.268 2.261 2.252 2.244 2.239 2.223 2.199 2.173 2.157 2.150 2.148 2.141 2.136 2.126 2.120 2.114 2.107 2.099 2.083 2.065 2.050 2.031 1.971 1.967 1.949 1.944 1.922 1.900 1.884 1.879 1.874 1.862 1.858 1.852 1.841 1.838 1.831 1.825 1.815 1.598 1.580 1.567 1.549

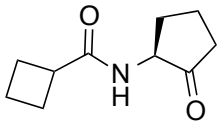

34

D1509080935_MEB_2.201_12-17.11.fid — Group Blackwell — C13CPD32 CDCl3 /home/mboursier/av400 mboursier 51

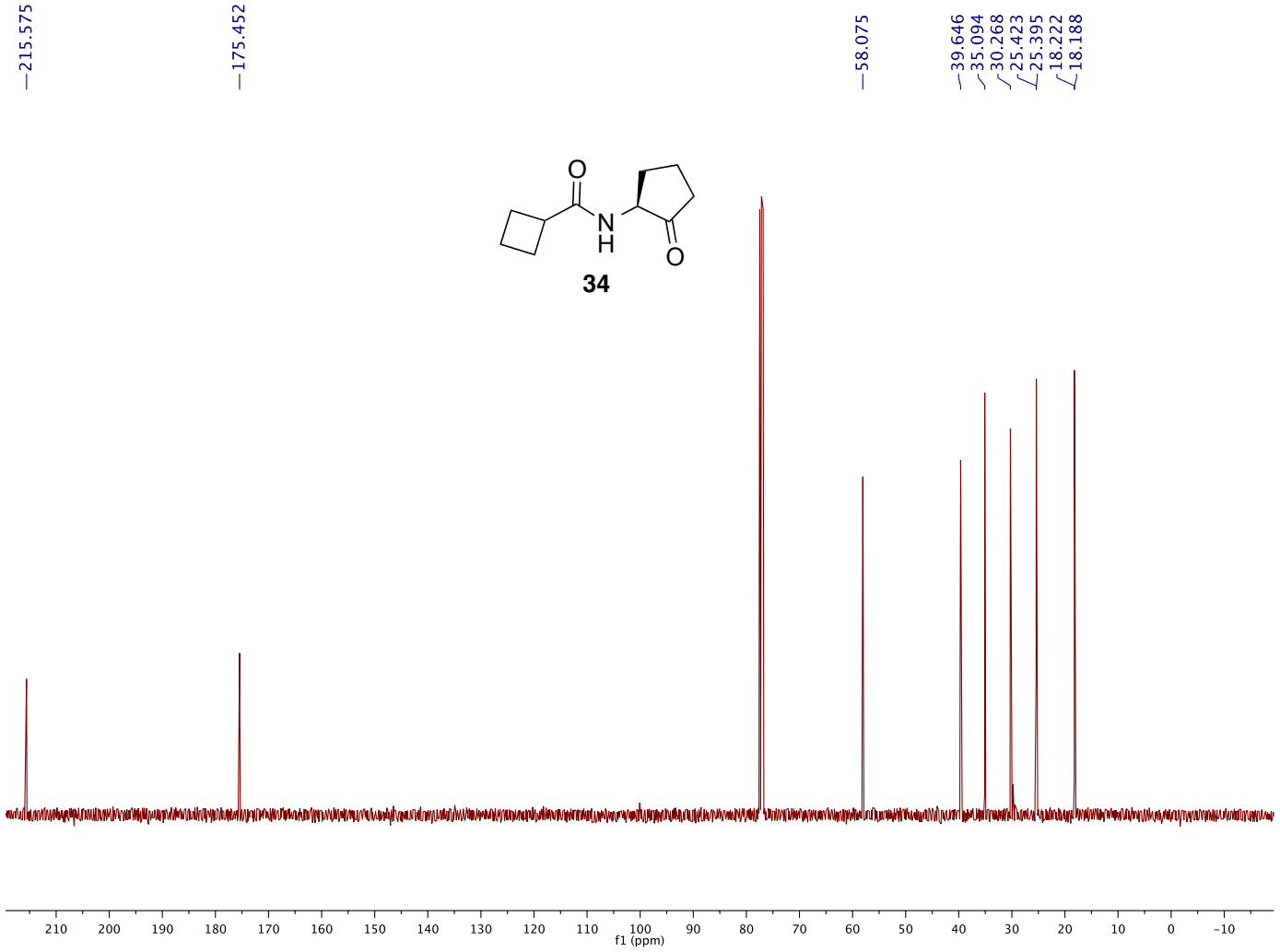

2.139 Pure — 400MHz, chloroform-d — 061815

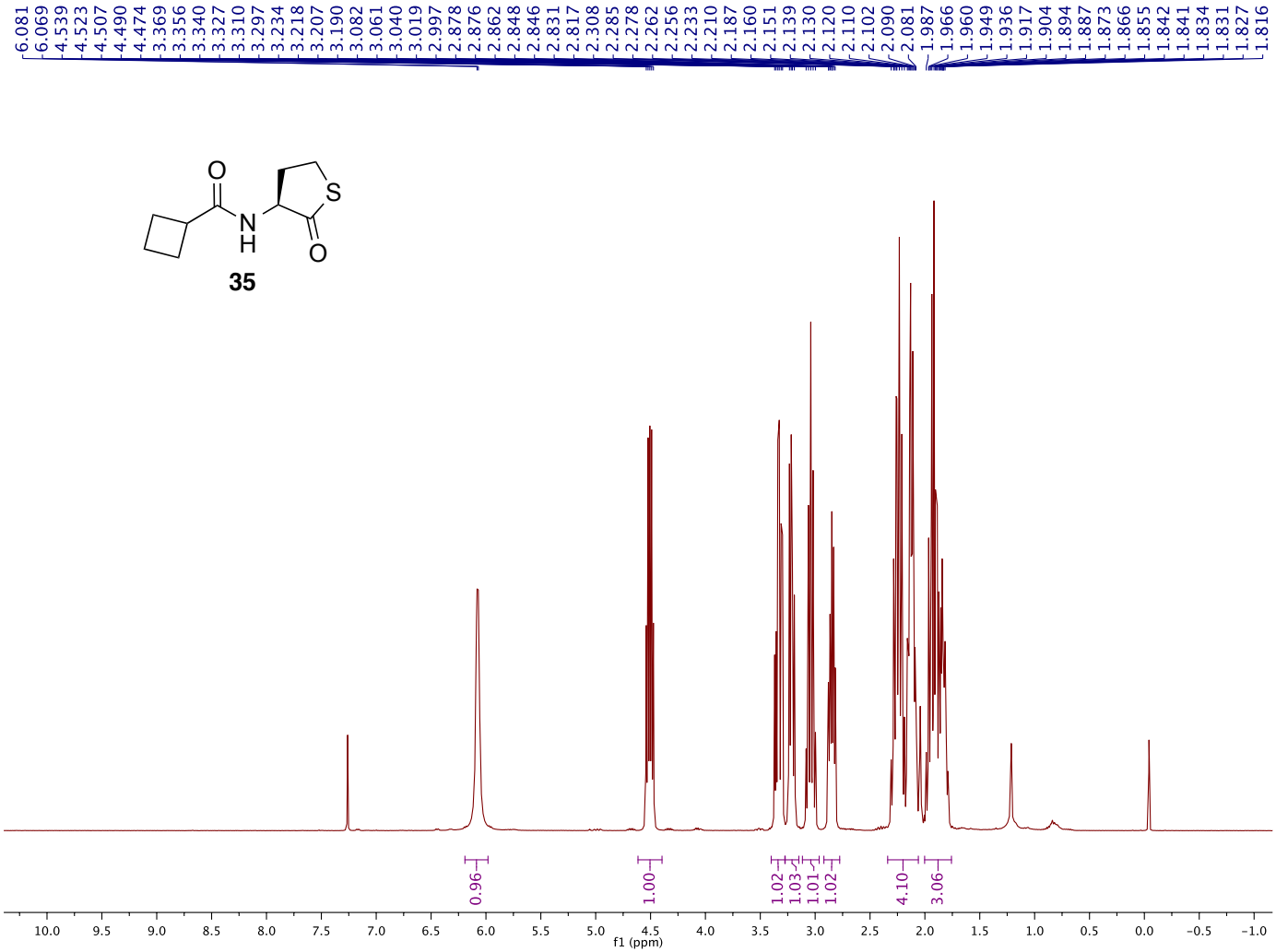

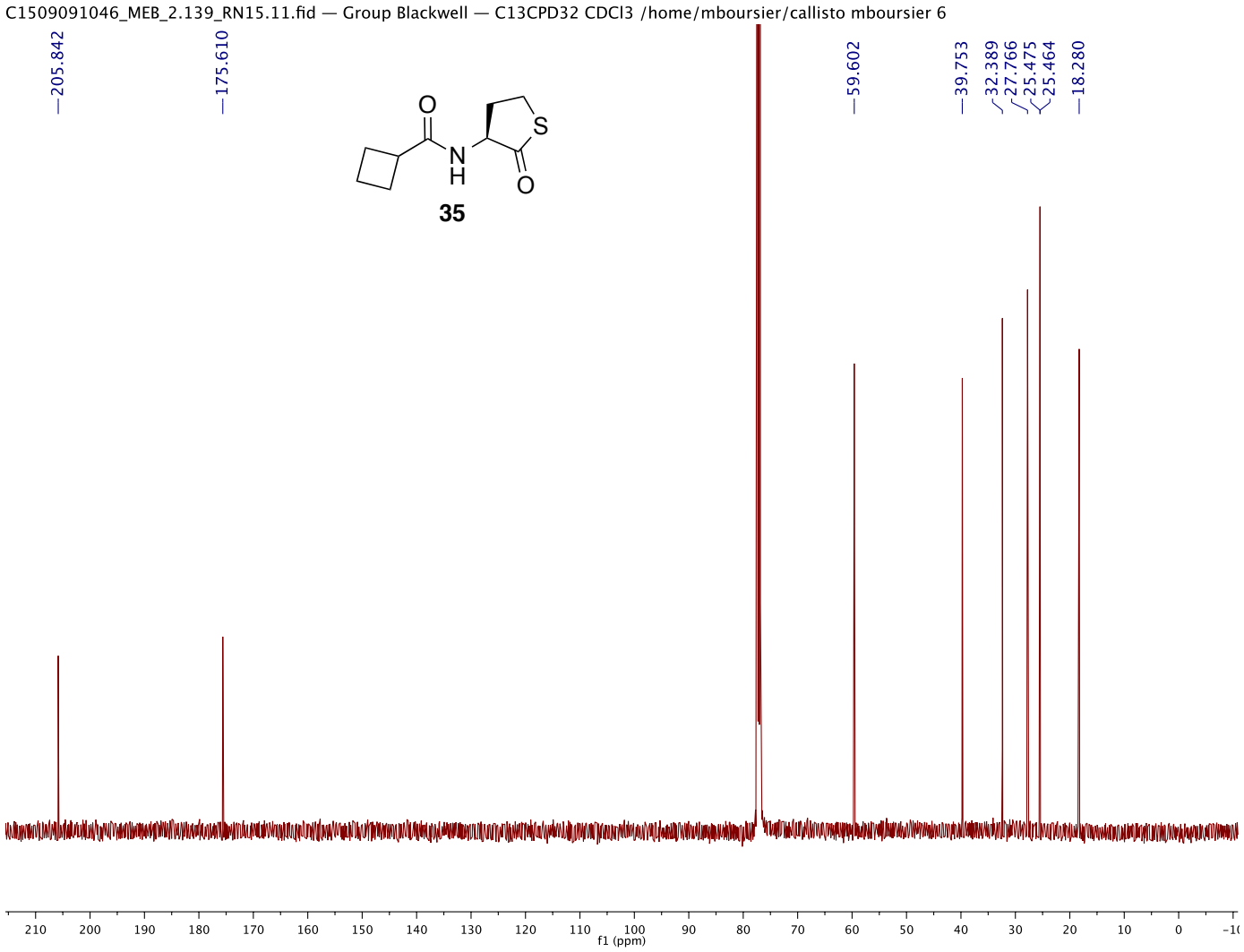
C1509091046_MEB_2.139_RN15.11.fid — Group Blackwell — C13CPD32 CDCl3 /home/mboursier/callisto mboursier 6
205.842
175.610
59.602
39.753
32.389
27.766
25.475
25.464
18.280
O
N
H
S
O
35
210 200 190 180 170 160 150 140 130 120 110 100 90 80 70 60 50 40 30 20 10 0
f1 (ppm)

C1606281816_RN19OH.10.fid — Group Blackwell — H1_standard.UW CDCl3 /home/mboursier/callisto mboursier 37

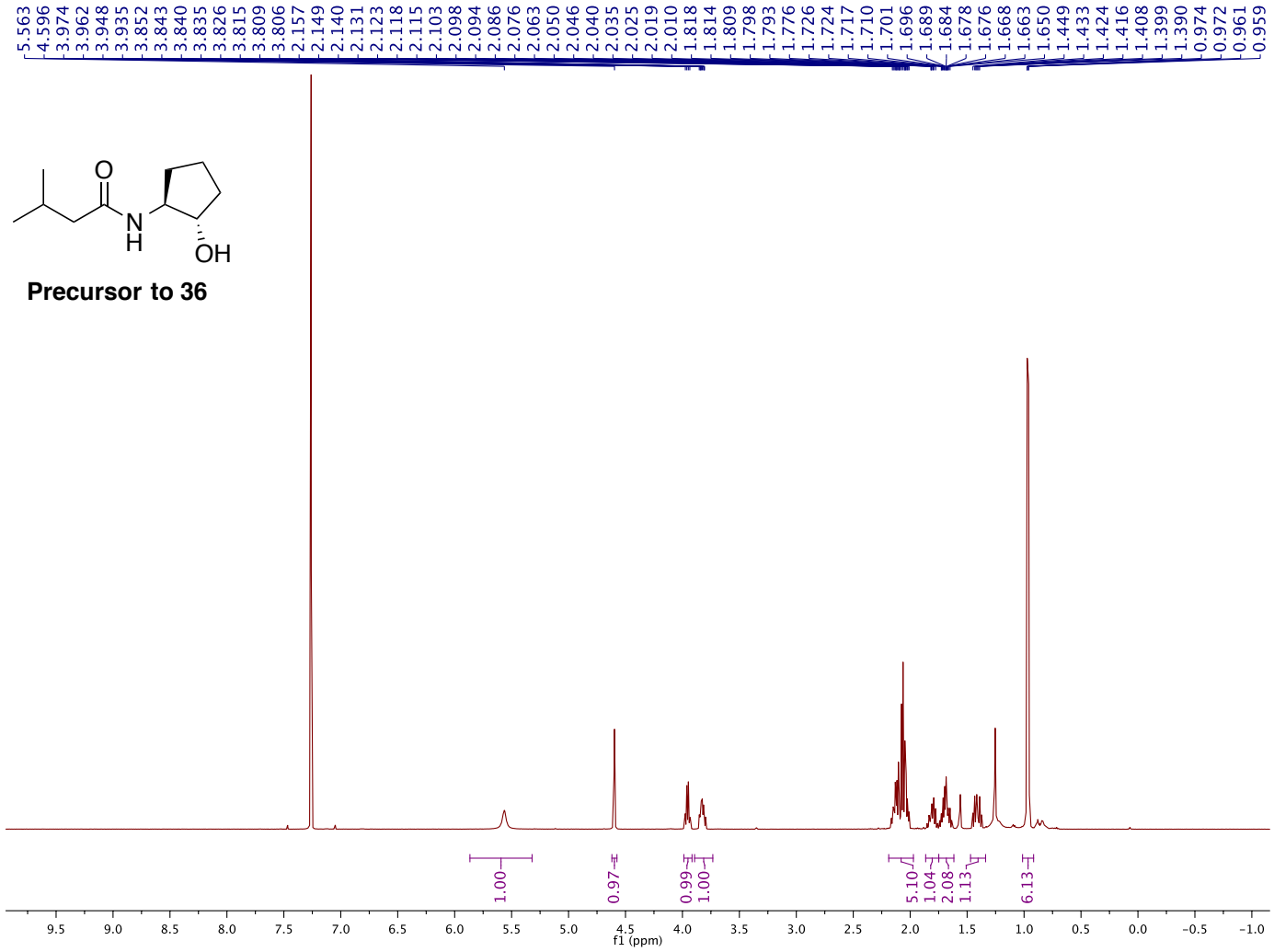

Precursor to 36

C1606281816_RN19OH.11.fid — Group Blackwell — C13_H1dec.UW CDCl3 /home/mboursier/callisto mboursier 37

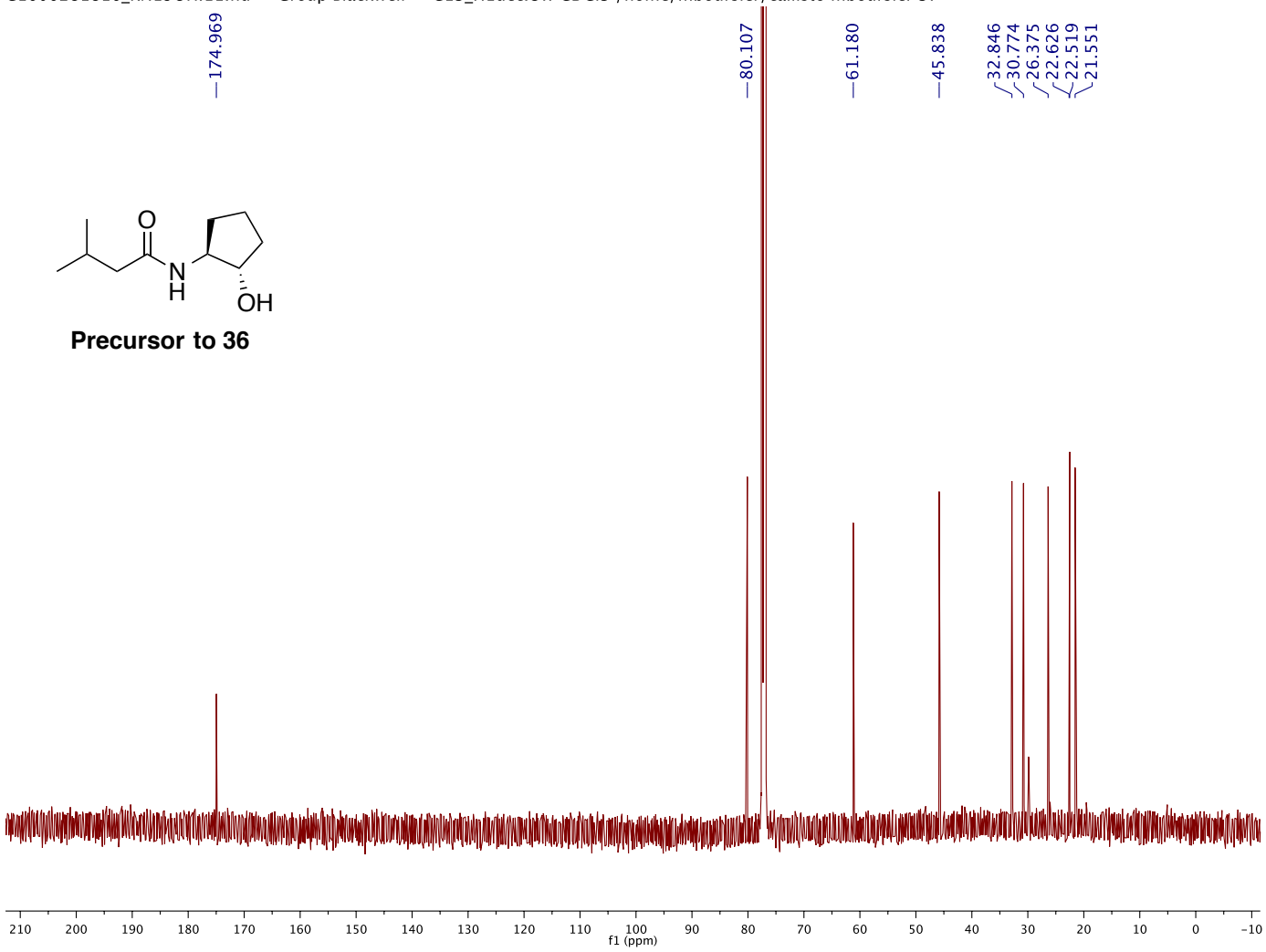

Precursor to 36

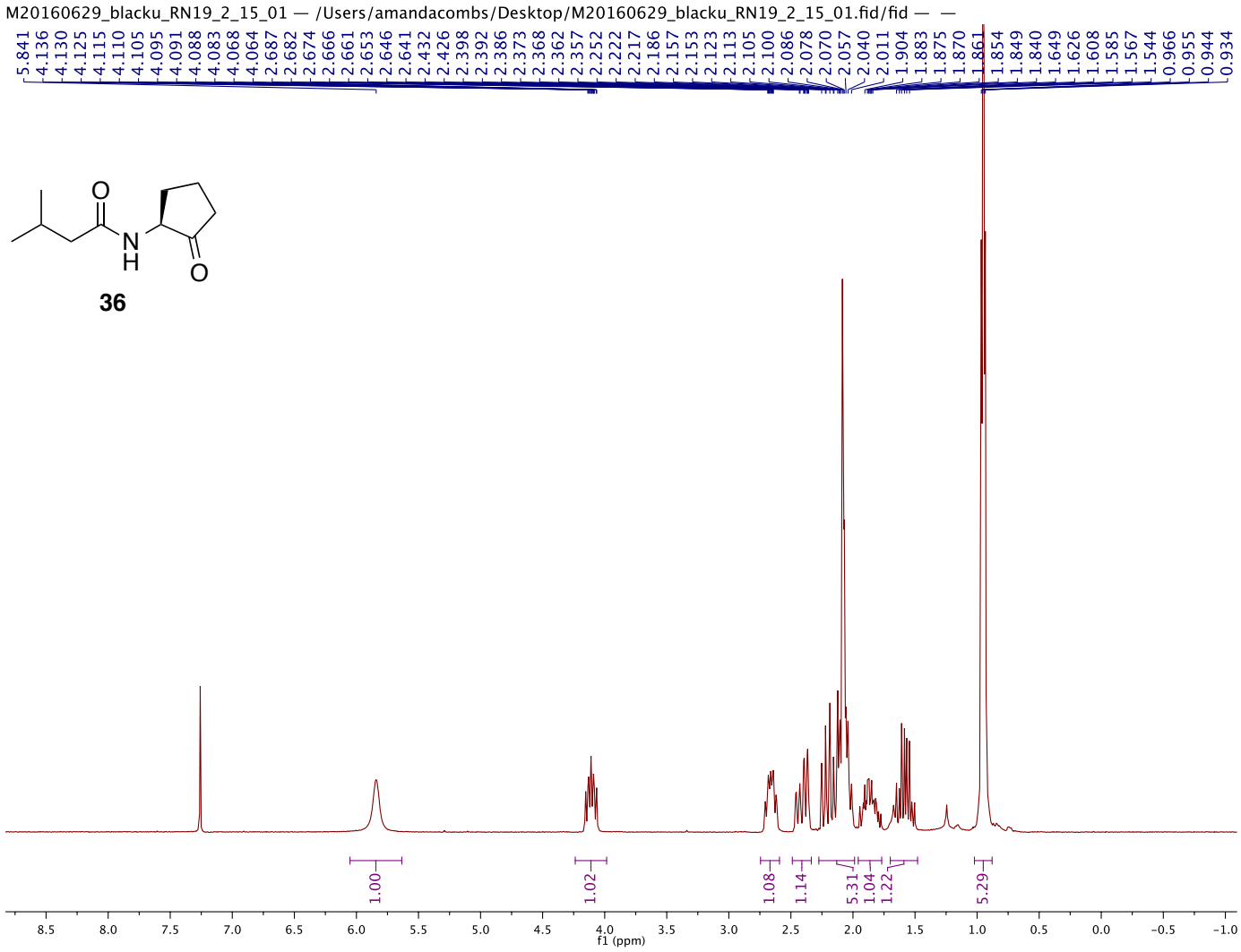
M20160629_blacku_RN19_2_15_01 — /Users/amandacombs/Desktop/M20160629_blacku_RN19_2_15_01.fid/fid — —
5.841
4.136
4.130
4.125
4.115
4.110
4.105
4.095
4.091
4.088
4.083
4.068
4.064
2.687
2.682
2.674
2.666
2.661
2.653
2.646
2.641
2.432
2.426
2.398
2.392
2.386
2.373
2.368
2.362
2.357
2.252
2.222
2.217
2.186
2.157
2.153
2.123
2.113
2.105
2.100
2.086
2.078
2.070
2.057
2.040
2.011
1.904
1.883
1.875
1.870
1.861
1.854
1.849
1.840
1.649
1.626
1.608
1.585
1.567
1.544
0.966
0.955
0.944
0.934
O
N
H
O
36
1.00
1.02
1.08
1.14
5.31
1.04
1.22
5.29
8.5
8.0
7.5
7.0
6.5
6.0
5.5
5.0
4.5
4.0
3.5
3.0
2.5
2.0
1.5
1.0
0.5
0.0
−0.5
−1.0
f1 (ppm)

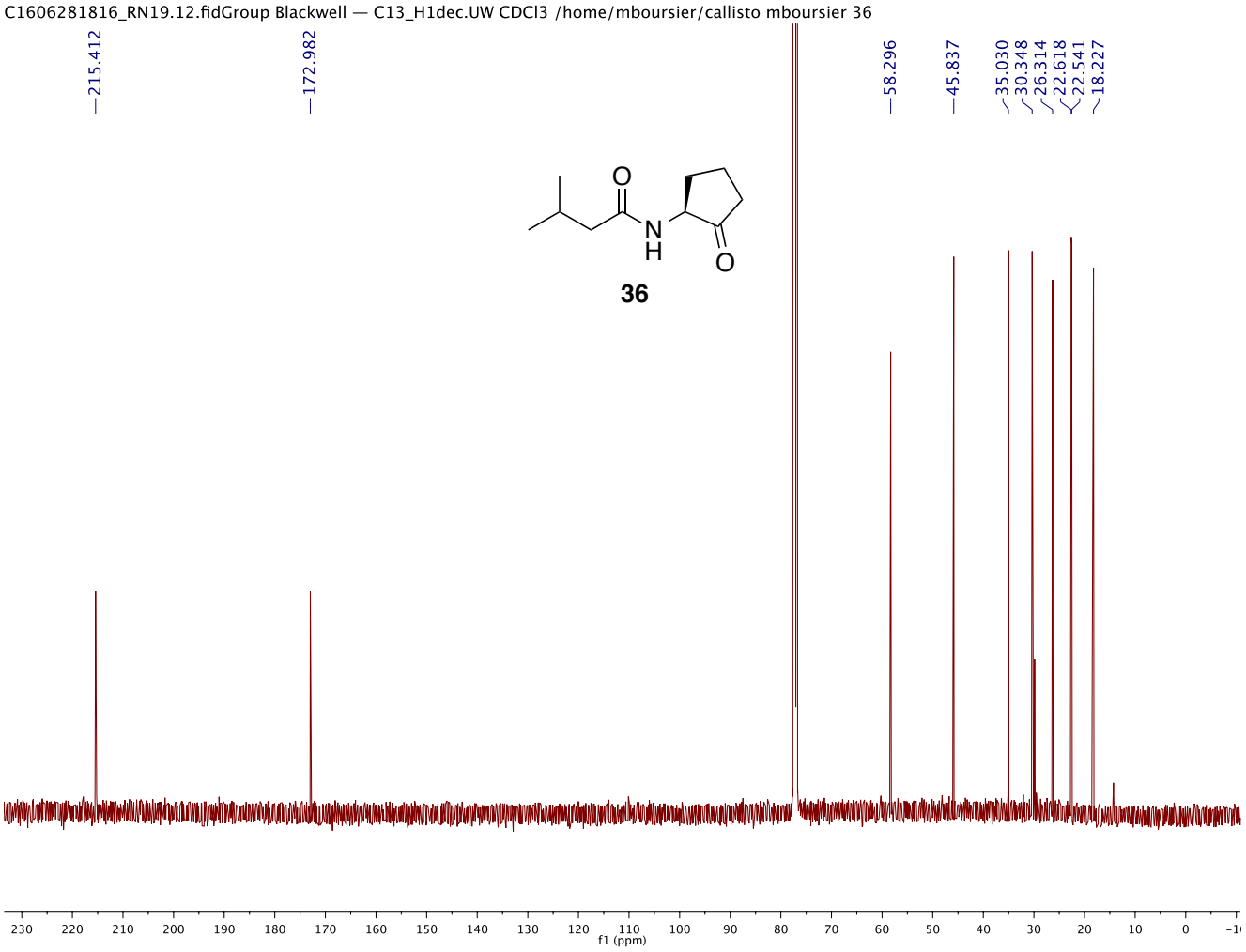
C1606281816_RN19.12.fidGroup Blackwell — C13_H1dec.UW CDCl3 /home/mboursier/callisto mboursier 36
215.412
172.982
58.296
45.837
35.030
30.348
26.314
22.618
22.541
18.227
O
N
H
O
36
230 220 210 200 190 180 170 160 150 140 130 120 110 100 90 80 70 60 50 40 30 20 10 0
f1 (ppm)

M20160413_mboursier_MEB_3_45_5-8_20_01

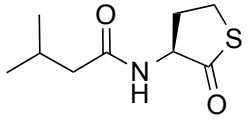

37

M20160413_mboursier_MEB_3_45_5-8carbon_20_01 — /Users/michelleboursier/Desktop/M20160413_mboursier_MEB_3_45_5-8carbon_20_01.fid/fid —

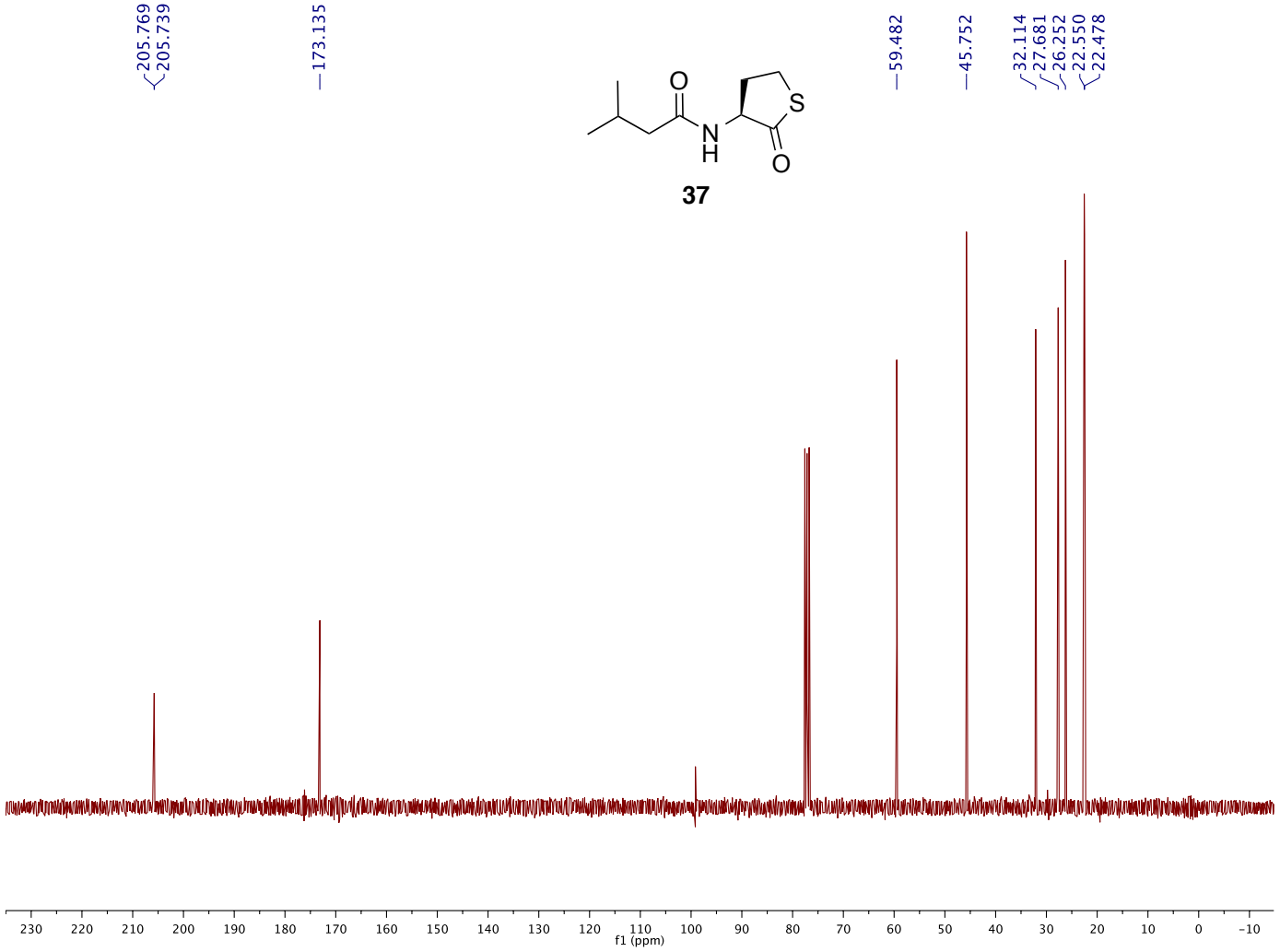

37

MEB 2.141P — 400MHz, chloroform-d — 062315

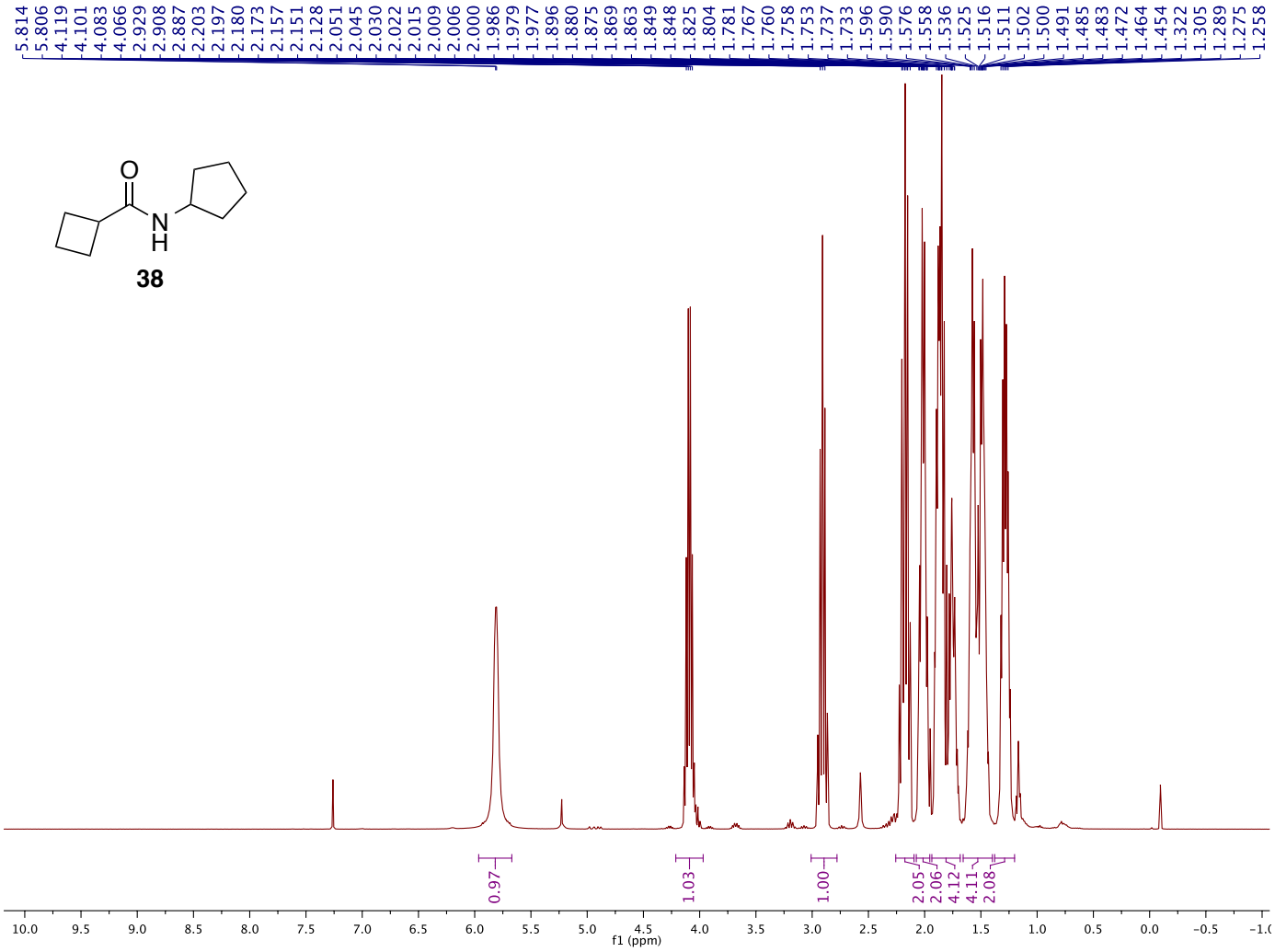

38

C1509091045_MEB_2.141_RN13.11.fid — Group Blackwell — C13CPD32 CDCl3 /home/mboursier/callisto mboursier 4

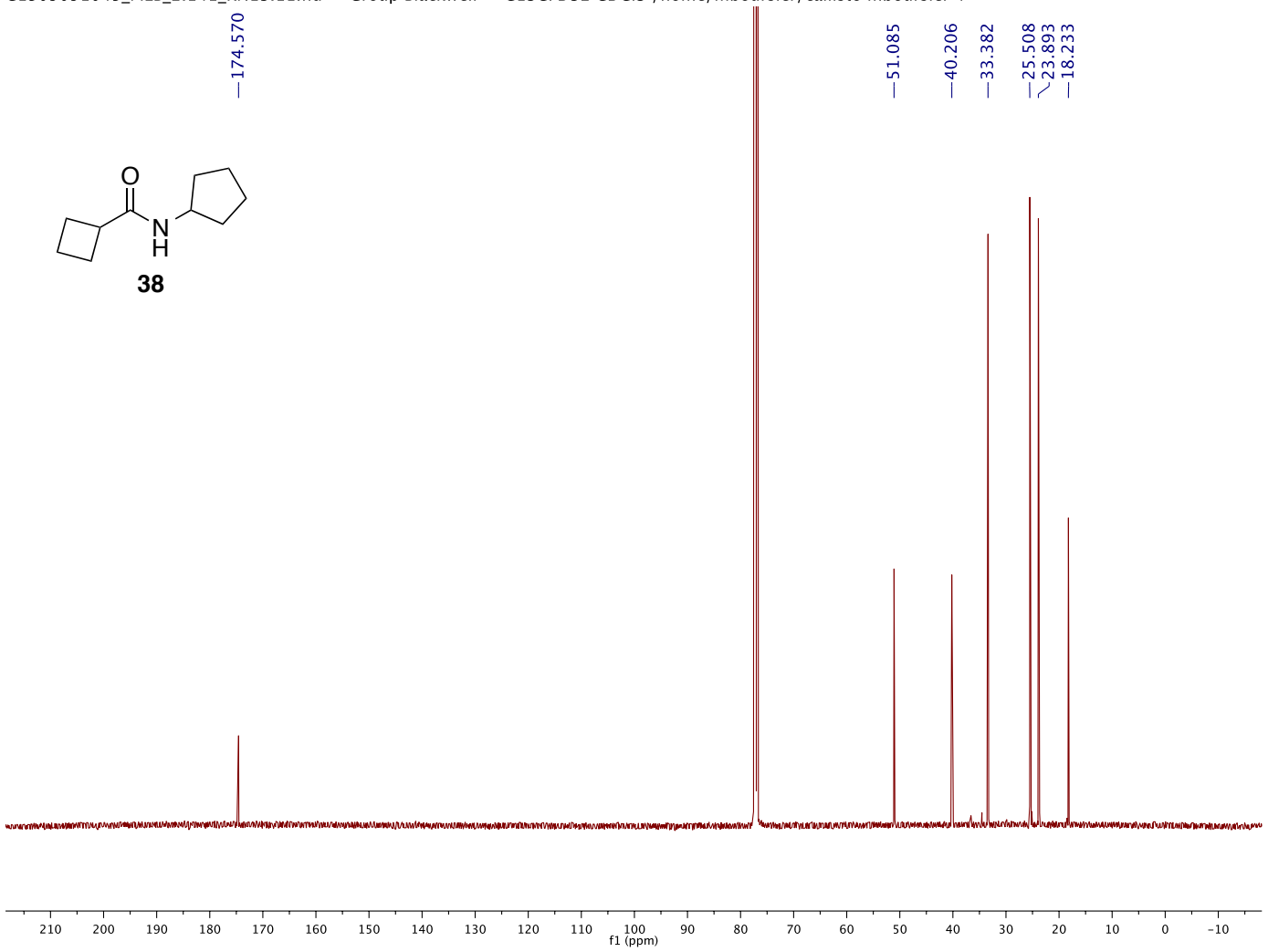

38

C1606281816_RN20.10.fid — Group Blackwell — H1_standard.UW CDCl3 /home/mboursier/callisto mboursier 38

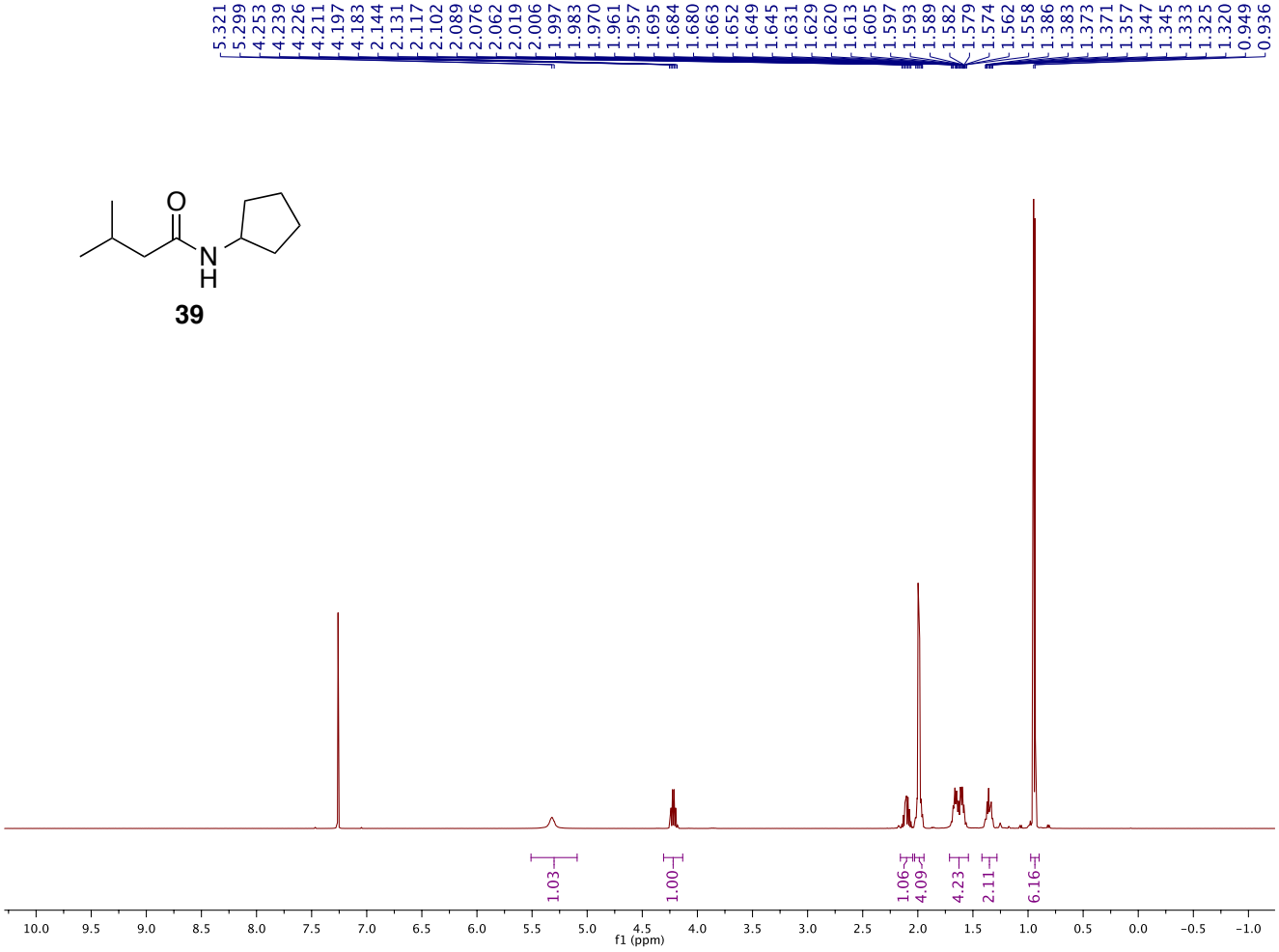

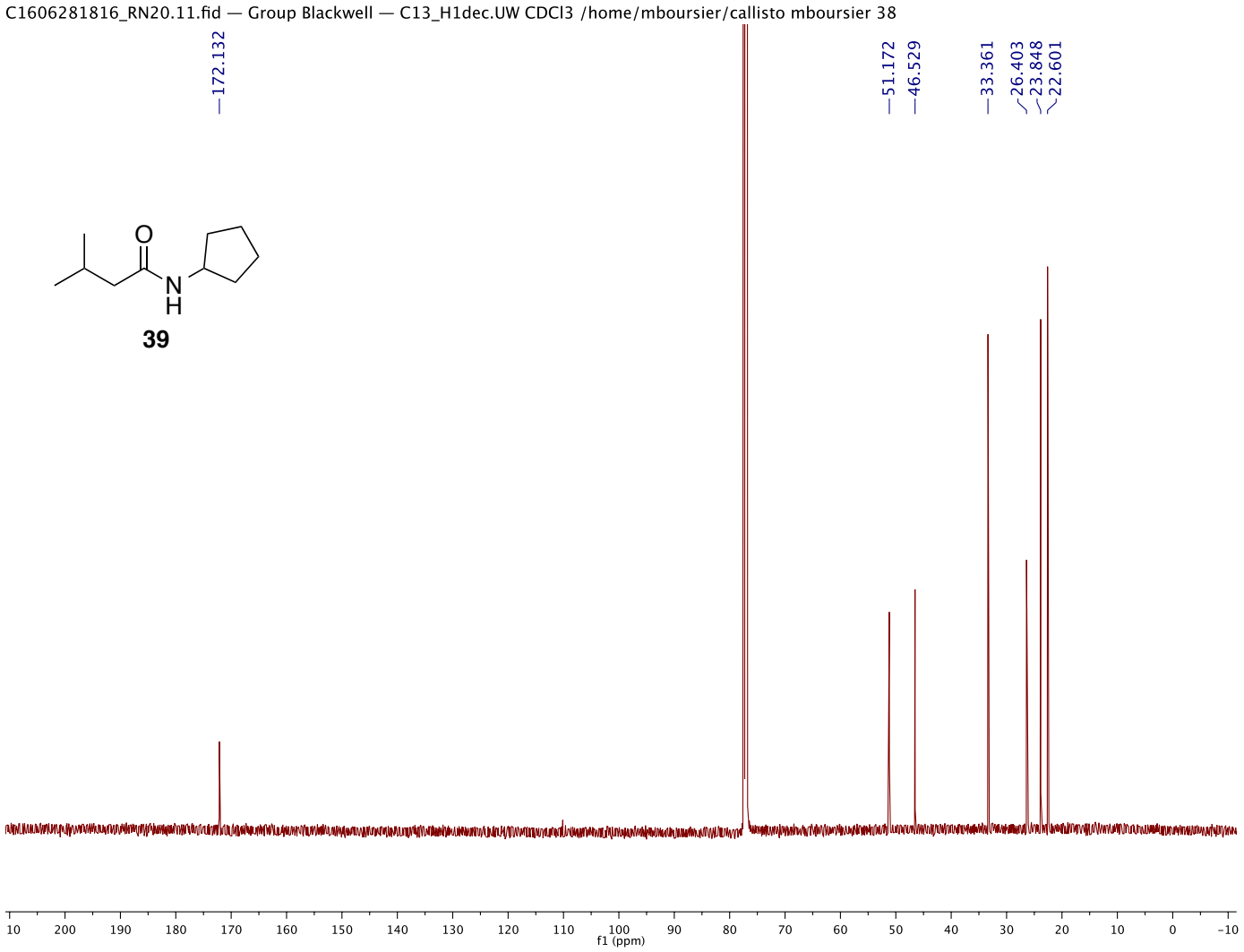
C1606281816_RN20.11.fid — Group Blackwell — C13_H1dec.UW CDCl3 /home/mboursier/callisto mboursier 38
172.132
51.172
46.529
33.361
26.403
23.848
22.601
O
N
H
39
10
200
190
180
170
160
150
140
130
120
110
100
90
80
70
60
50
40
30
20
10
0
−10
f1 (ppm)

D1604141010_MEB_3.40RC.10.fid — Group Blackwell — H1_standard.UW CDCl3 /home/mboursier/av400 mboursier 70

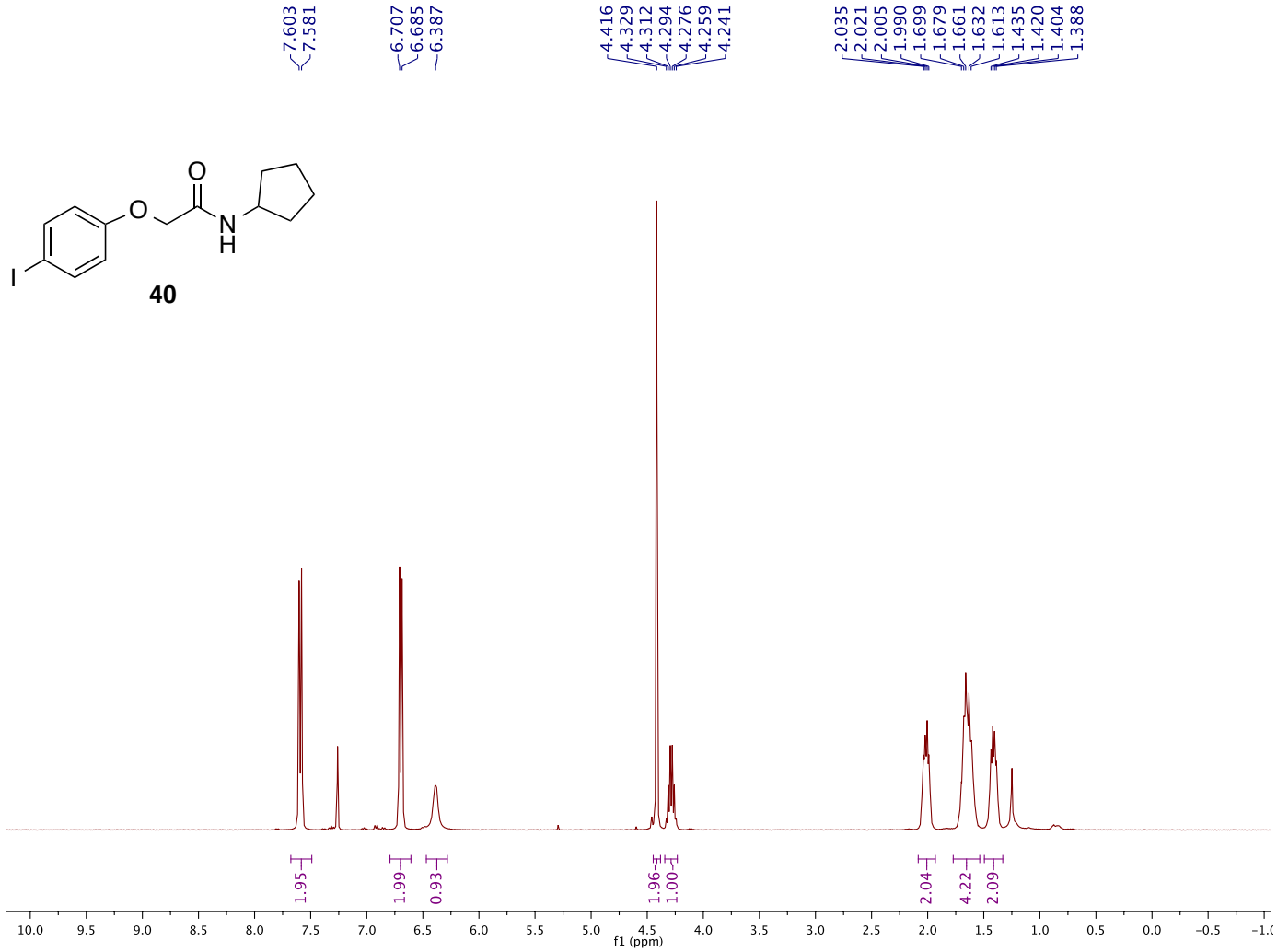

D1604051538_MEB_3.40P.11.fid — Group Blackwell — C13_H1dec.UW CDCl3 /home/mboursier/av400 mboursier 70

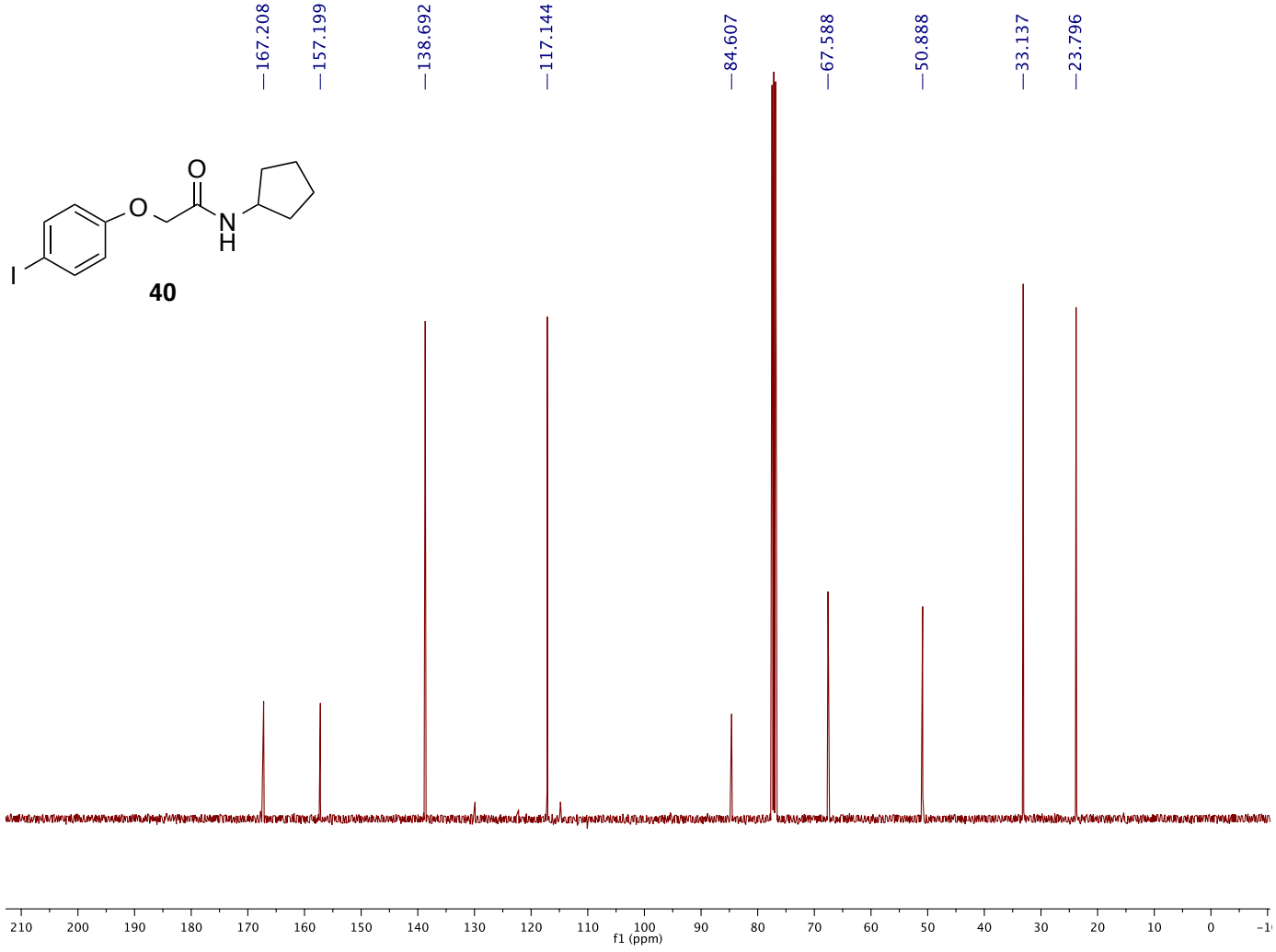

C1606281816_RN21.10.fid — Group Blackwell — H1_standard.UW CDCl3 /home/mboursier/callisto mboursier 39

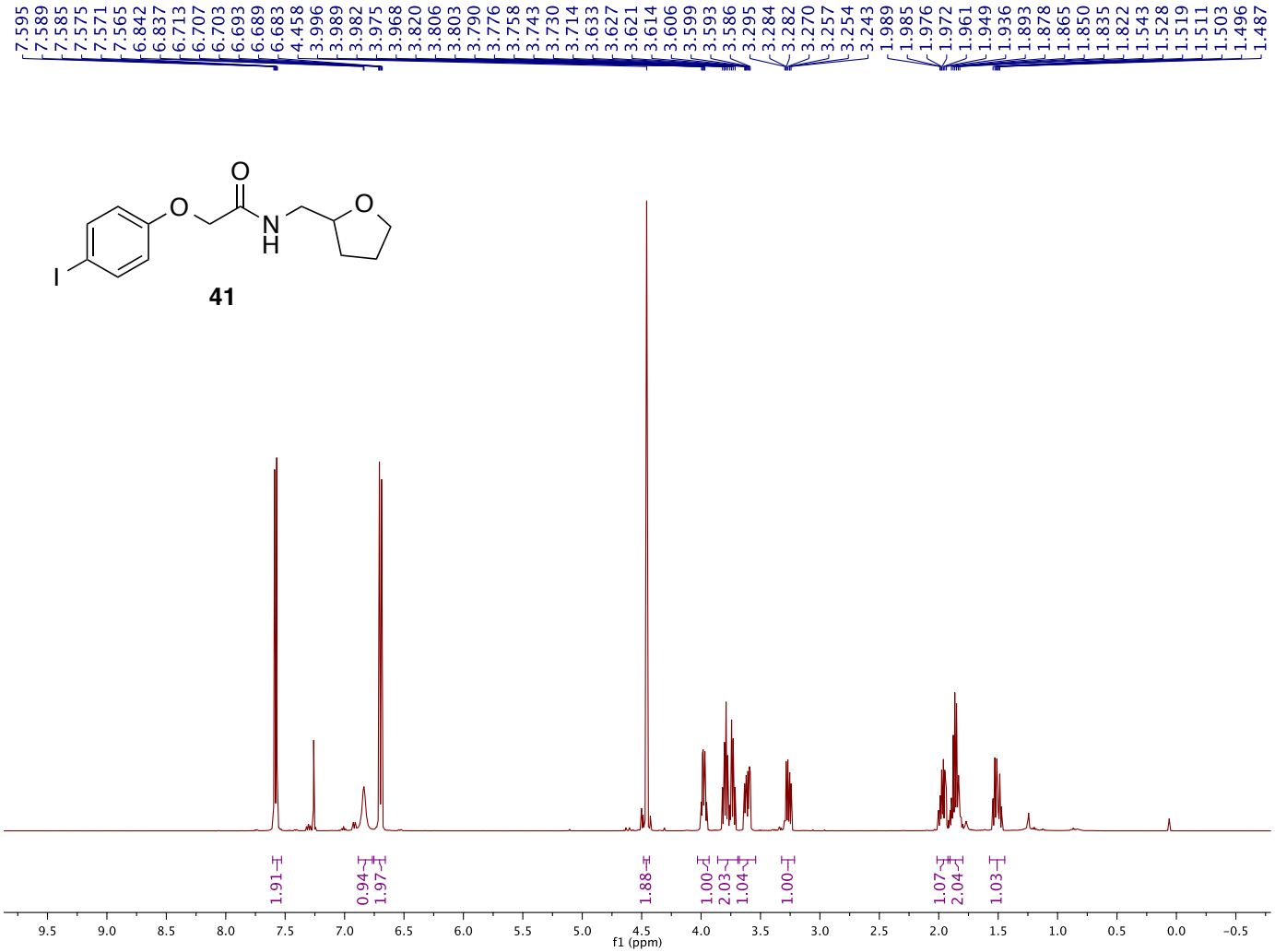

C1606281816_RN21.11.fid — Group Blackwell — C13_H1dec.UW CDCl3 /home/mboursier/callisto mboursier 39

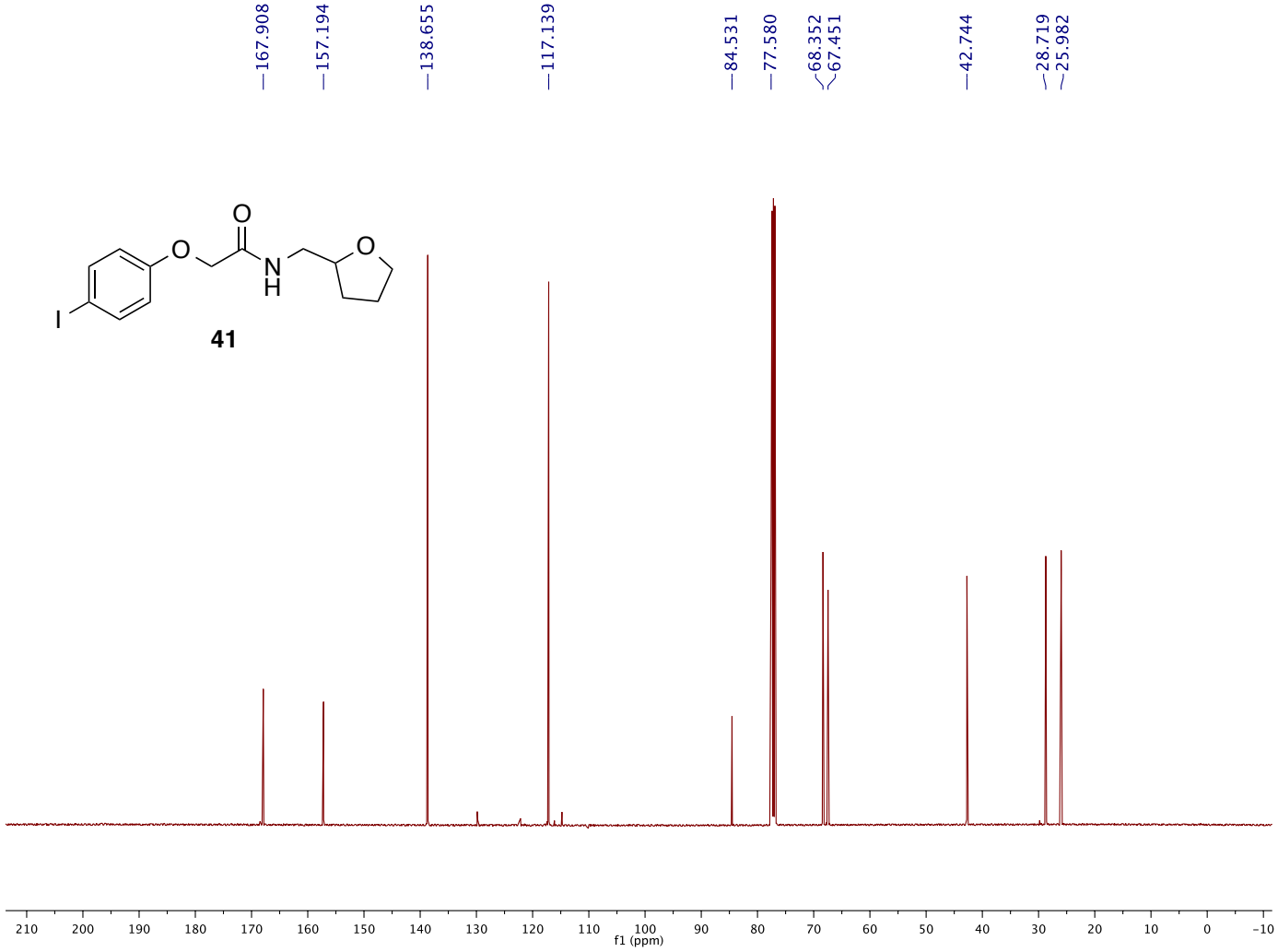

C1606281816_RN22.10.fid — Group Blackwell — H1_standard.UW CDCl3 /home/mboursier/callisto mboursier 40

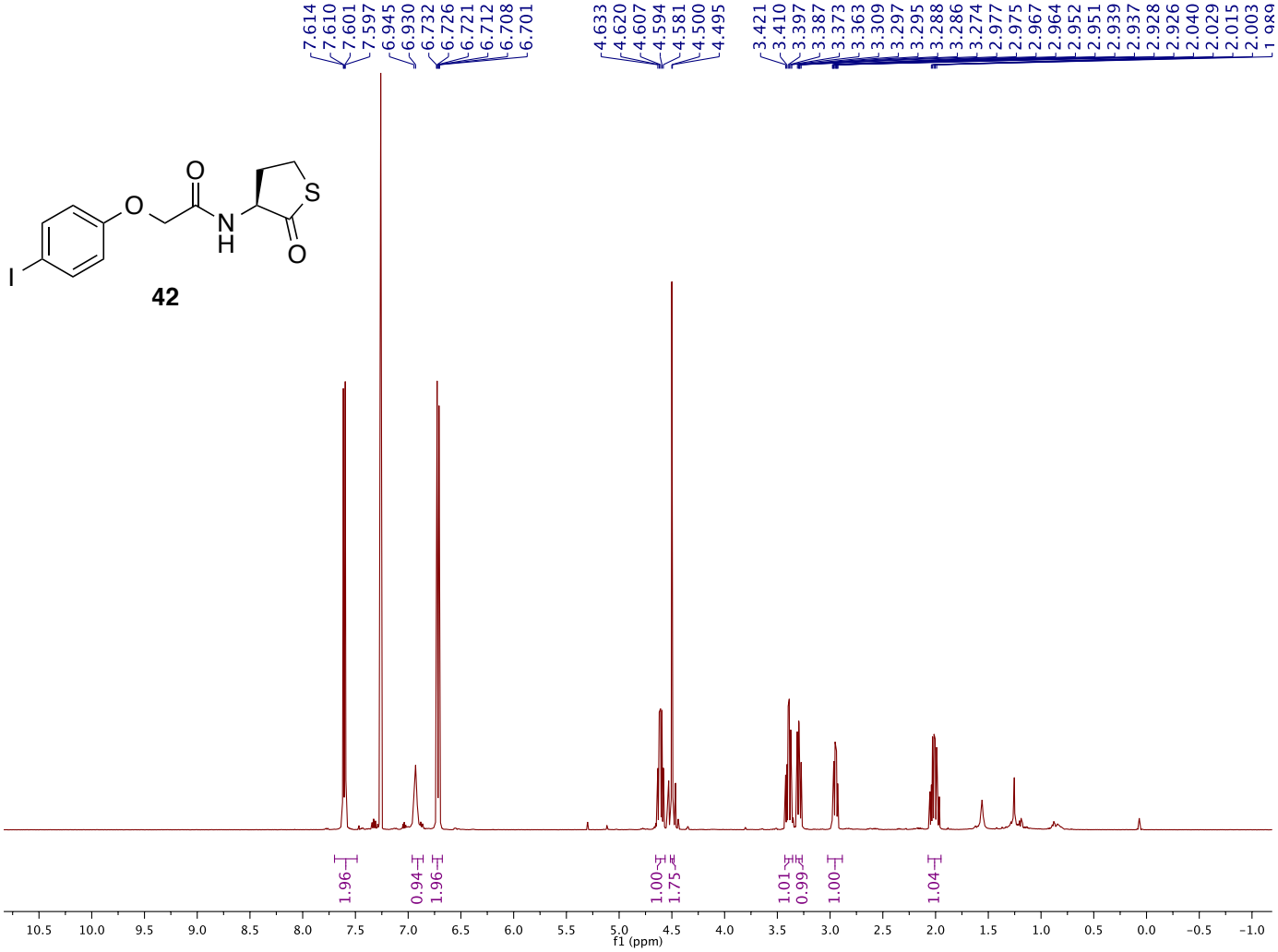

C1606281816_RN22.11.fid — Group Blackwell — C13_H1dec.UW CDCl3 /home/mboursier/callisto mboursier 40

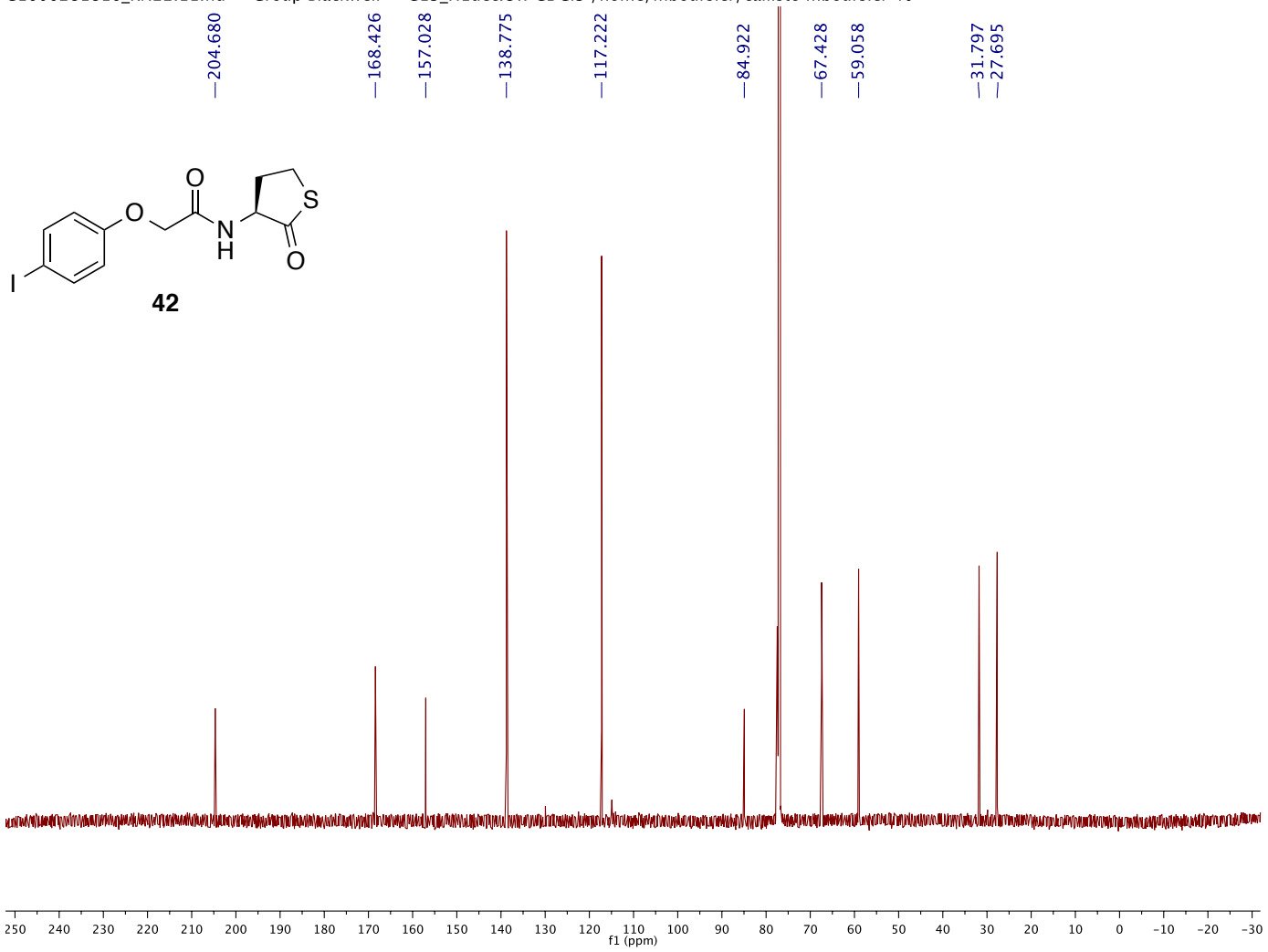

References

1. O'Reilly, M. C., and Blackwell, H. E. (2016) Structure-Based Design and Biological Evaluation of Triphenyl Scaffold-Based Hybrid Compounds as Hydrolytically Stable Modulators of a LuxR-Type Quorum Sensing Receptor, *ACS Infect. Dis. 2*, 32-38.

2. Zirvi, K. A., and Jarboe, C. H. (1971) Infrared Spectral Characteristics of the Cyclobutane Ring System, *J. Chem. Soc. B*, 1603-1606.

3. Prinz, H. (2010) Hill coefficients, dose-response curves and allosteric mechanisms, *J. Chem. Biol. 3*, 37-44.

4. Eibergen, N. R., Moore, J. D., Mattmann, M. E., and Blackwell, H. E. (2015) Potent and Selective Modulation of the RhlR Quorum Sensing Receptor by Using Non-native Ligands: An Emerging Target for Virulence Control in *Pseudomonas aeruginosa*, *ChemBioChem 16*, 2348-2356.

5. Moore, J. D., Rossi, F. M., Welsh, M. A., Nyffeler, K. E., and Blackwell, H. E. (2015) A Comparative Analysis of Synthetic Quorum Sensing Modulators in *Pseudomonas aeruginosa*: New Insights into Mechanism, Active Efflux Susceptibility, Phenotypic Response, and Next-Generation Ligand Design, *J. Am. Chem. Soc. 137*, 14626-14639.